

11-29-2022

Synaptic Development in Diverse Olfactory Neuron Classes Uses Distinct Temporal and Activity-Related Programs

Michael A. Aimino
Thomas Jefferson University

Alison T. DePew
Thomas Jefferson University

Lucas Restrepo
Thomas Jefferson University

Timothy J. Mosca
Thomas Jefferson University

Follow this and additional works at: <https://jdc.jefferson.edu/farberneursofp>

 Part of the [Medical Neurobiology Commons](#), and the [Neurosciences Commons](#)


[Let us know how access to this document benefits you](#)

Recommended Citation

Aimino, Michael A.; DePew, Alison T.; Restrepo, Lucas; and Mosca, Timothy J., "Synaptic Development in Diverse Olfactory Neuron Classes Uses Distinct Temporal and Activity-Related Programs" (2022). *Farber Institute for Neuroscience Faculty Papers*. Paper 46.
<https://jdc.jefferson.edu/farberneursofp/46>

This Article is brought to you for free and open access by the Jefferson Digital Commons. The Jefferson Digital Commons is a service of Thomas Jefferson University's [Center for Teaching and Learning \(CTL\)](#). The Commons is a showcase for Jefferson books and journals, peer-reviewed scholarly publications, unique historical collections from the University archives, and teaching tools. The Jefferson Digital Commons allows researchers and interested readers anywhere in the world to learn about and keep up to date with Jefferson scholarship. This article has been accepted for inclusion in Farber Institute for Neuroscience Faculty Papers by an authorized administrator of the Jefferson Digital Commons. For more information, please contact: JeffersonDigitalCommons@jefferson.edu.

Synaptic Development in Diverse Olfactory Neuron Classes Uses Distinct Temporal and Activity-Related Programs

Michael A. Aimino, Alison T. DePew, Lucas Restrepo, and  Timothy J. Mosca

Department of Neuroscience, Vickie and Jack Farber Institute of Neuroscience, Thomas Jefferson University, Philadelphia, Pennsylvania 19107

Developing neurons must meet core molecular, cellular, and temporal requirements to ensure the correct formation of synapses, resulting in functional circuits. However, because of the vast diversity in neuronal class and function, it is unclear whether or not all neurons use the same organizational mechanisms to form synaptic connections and achieve functional and morphologic maturation. Moreover, it remains unknown whether neurons united in a common goal and comprising the same sensory circuit develop on similar timescales and use identical molecular approaches to ensure the formation of the correct number of synapses. To begin to answer these questions, we took advantage of the *Drosophila* antennal lobe (AL), a model olfactory circuit with remarkable genetic access and synapse-level resolution. Using tissue-specific genetic labeling of active zones, we performed a quantitative analysis of synapse formation in multiple classes of neurons of both sexes throughout development and adulthood. We found that olfactory receptor neurons (ORNs), projection neurons (PNs), and local interneurons (LNs) each have unique time courses of synaptic development, addition, and refinement, demonstrating that each class follows a distinct developmental program. This raised the possibility that these classes may also have distinct molecular requirements for synapse formation. We genetically altered neuronal activity in each neuronal subtype and observed differing effects on synapse number based on the neuronal class examined. Silencing neuronal activity in ORNs, PNs, and LNs impaired synaptic development but only in ORNs did enhancing neuronal activity influence synapse formation. ORNs and LNs demonstrated similar impairment of synaptic development with enhanced activity of a master kinase, GSK-3 β , suggesting that neuronal activity and GSK-3 β kinase activity function in a common pathway. ORNs also, however, demonstrated impaired synaptic development with GSK-3 β loss-of-function, suggesting additional activity-independent roles in development. Ultimately, our results suggest that the requirements for synaptic development are not uniform across all neuronal classes with considerable diversity existing in both their developmental time frames and molecular requirements. These findings provide novel insights into the mechanisms of synaptic development and lay the foundation for future work determining their underlying etiologies.

Key words: antennal lobe; CNS; development; *Drosophila*; olfaction; synapse

Significance Statement

Distinct olfactory neuron classes in *Drosophila* develop a mature synaptic complement over unique timelines and using distinct activity-dependent and molecular programs, despite having the same generalized goal of olfactory sensation.

Received May 12, 2022; revised Oct. 18, 2022; accepted Nov. 2, 2022.

Author contributions: M.A.A. and T.J.M. designed research; M.A.A., A.T.D., L.R., and T.J.M. performed research; M.A.A., A.T.D., L.R., and T.J.M. analyzed data; M.A.A. and T.J.M. wrote the first draft of the paper; M.A.A., A.T.D., and T.J.M. edited the paper; M.A.A. and T.J.M. wrote the paper.

This work was supported by National Institute of Health Grants R00-DC013059 and R01-NS110907 and the Commonwealth Universal Research Enhancement (CURE) Program of the Pennsylvania Department of Health Grant 4100077067 (to T.J.M.). Aspects of this work, as well as general work in the T.J.M. Lab are supported by grants from the Alfred P. Sloan Foundation, the Whitehall Foundation, the Jefferson Dean's Transformational Science Award, the Jefferson Synaptic Biology Center, and Thomas Jefferson University start-up funds. We thank Dr. Michael Parisi, Dr. Kristen Davis, Dr. Juan Carlos Duhart, Dr. Stephen Tymanskyj, Jesse Humenik, Dr. Le Ma, and S. Zosimus for stimulating discussions and comments on the manuscript. We also thank the Bloomington Stock Center for flies and the Developmental Studies Hybridoma Bank (University of Iowa, created by the National Institute of Child Health and Human Development) for antibodies.

L. Restrepo's present address: University of Massachusetts Chan Medical School, Department of Molecular, Cell, and Cancer Biology, Worcester MA, 01605.

The authors declare no competing financial interests.

Correspondence should be addressed to Timothy J. Mosca at timothy.mosca@jefferson.edu.

<https://doi.org/10.1523/JNEUROSCI.0884-22.2022>

Copyright © 2023 the authors

Introduction

Neuronal development is a complex, multistep process that must occur over a specific time frame and under precise conditions to produce a functioning nervous system. One crucial stage of this process is the formation of synapses (Lin and Goodman, 1994; Dalva et al., 2007; Siddiqui and Craig, 2011; Wilson, 2013; Mosca and Luo, 2014; de Ramon Francàs et al., 2017). Synaptic connections between neurons enable communication between cells as well as the processing of information to generate behavioral outputs (Farhy-Tselnicker and Allen, 2018). Despite having the same core function of synaptic communication, there is a vast diversity of neuron types in the nervous system (Masland, 2004; Zeng and Sanes, 2017; Wilton et al., 2019), and it is unclear whether all neurons follow the same time course of, and rely on the same molecular pathways and mechanisms, completing synapse formation. Because different regions of the nervous system, such as the peripheral nervous system or the CNS, develop over

different time frames and under different conditions (Baines and Bate, 1998; Li et al., 2010; Farhy-Tselnicker and Allen, 2018; Liu and Chakkalakal, 2018), it is likely that variations in synaptic development exist based on neuron type. Historically, much of our understanding of synapse formation has come from the neuromuscular junction (NMJ); the NMJ in particular has been essential in providing early insight into receptor structure, the calcium hypothesis of neurotransmitter release, and spontaneous neurotransmission as well as the basic elements of synaptogenic signals like Agrin (Nitkin et al., 1987; Sanes and Lichtman, 1999; Kummer et al., 2006; Wu et al., 2010; Shi et al., 2012; Li et al., 2018). Many of the molecular mechanisms that regulate NMJ synapse formation are also found in the CNS, but a thorough understanding is currently lacking and it remains unknown whether peripheral synaptic mechanisms are fully conserved with those that govern central synapse development and organization (Keshishian et al., 1996; Goda and Davis, 2003; Collins and DiAntonio, 2007; DePew et al., 2019; DePew and Mosca, 2021). It is further unclear whether all CNS neuron types follow the same rules for synapse formation given the considerable complexity of neuronal class, morphology, synaptic organization, and functional properties (including release probability, safety factor, firing frequency, etc.) in the brain. Therefore, it is critical to determine the basic temporal and molecular characteristics of synapse development within central circuits and to understand how different potential mechanisms of development influence the diversity of synaptic organization in mature neurons. Knowing the general rules of normal development will inform our perspective on how defects during development can lead to neurodevelopmental and neurologic disorders associated with synapse dysfunction such as autism, schizophrenia, or epilepsy (Bennett, 2011; Grant, 2012; Bonansco and Fuenzalida, 2016; Mullins et al., 2016). Further, there is considerable evidence that different neurologic and neurodegenerative disorders, such as Parkinson's disease or amyotrophic lateral sclerosis, specifically affect distinct populations of neurons over others (Ilieva et al., 2009; Dabool et al., 2019). The underlying basis for this selectivity remains unknown but understanding the functional, molecular, and developmental differences between different neuron types may provide unique insight into their vulnerability, or resistance, to such disease mechanisms.

The *Drosophila* antennal lobe (AL) represents a powerful model system for understanding the circuit-level, synaptic, and molecular aspects of how individual neuronal classes in a network undergo synaptic development (Jefferis and Hummel, 2006; Hummel and Rodrigues, 2008; Wilson, 2013; Mosca and Luo, 2014; Grabe et al., 2016; Seki et al., 2017). In *Drosophila*, olfaction is a guiding sensory modality, enabling flies to find food or mates, avoid danger, and communicate (Hildebrand and Shepherd, 1997; Grabe and Sachse, 2018). The AL is the first order olfactory structure in the fly brain (Stocker et al., 1990; Couto et al., 2005; Fishilevich and Vosshall, 2005) and is the essential gatekeeper of all olfactory information to higher brain centers. The AL is functionally analogous to the mammalian olfactory bulb (Wilson, 2013; Sakano, 2020) and represents a simple sensory circuit in which each neuron class is genetically accessible and current imaging technologies enable high-resolution analysis with synaptic resolution (Wilson, 2013; Mosca and Luo, 2014; Li et al., 2020). Moreover, because of the high throughput nature of the system, different developmental stages are easily studied across multiple animals to examine stereotypy and variability during development. Taken together, current abilities enable a quantitative, temporal comparison of synapse development in AL neurons by visualizing the relative number of

active zones, the sites of neurotransmitter release, in a single neuronal class and among different neuronal classes in the same sensory circuit. The multiple types of neurons found within the AL each have their own specific function, but also possess the shared goal of interpreting olfactory information to achieve a proper behavioral output. Olfactory receptor neurons (ORNs) comprise the primary sensory neuron population and receive input in the form of olfactory stimuli, detected from the outside environment, through the antennae and maxillary palps (Vosshall et al., 2000). Projection neurons (PNs) receive input from ORNs via dendritic terminals in the antennal lobe and project information to higher order olfactory centers like the mushroom body and the lateral horn via axon terminals (Modi et al., 2020) to result in a behavioral output (Jefferis et al., 2001). PNs also form dendrodendritic synapses with other PNs and synapse onto a third class of cells, the local interneurons (LNs). LNs form synapses with ORNs and other LNs throughout the ALs to regulate gain control of the olfactory signals, completing and refining the circuit (Tanaka et al., 2009; Yaksi and Wilson, 2010). The three main neuronal classes of the AL have clearly defined roles, but all interact to achieve the goal of odorant sensation. ORNs, PNs, and LNs thus comprise a complex, but tractable, sensory circuit suited to high-resolution synaptic and developmental analyses (Fig. 1A). We sought to compare the temporal and molecular programs that ORNs, PNs, and LNs employ to accomplish synaptic development.

In this study, we mapped synaptic development in identified, genetically accessible classes of ORNs, PNs, and LNs across both sexes from early pupal development to mature adulthood in the *Drosophila* AL, creating the first, detailed, time course of synaptic development in individual olfactory neuron populations. We found that ORNs, PNs, and LNs each have a distinct pattern of synaptic development, including periods of synaptic addition, removal or pruning stages, and synapse loss in late adulthood. We also determined that different subclasses of ORNs use different temporal programs of synaptic development based on their preferred odorant type, such as odors for food or pheromones, or sexual dimorphism. Having established distinct timelines of synapse addition and pruning that culminate in mature synaptic organization for each class of AL neurons, we examined how activity influenced mature synapse number after development in ORNs, PNs, and LNs. Intriguingly, beyond the temporal differences in synaptic development, we also determined that each class of AL neurons responded differently to perturbations in neuronal activity. When synaptic transmission was blocked or neuronal excitability decreased cell-autonomously, ORNs, PNs, and LNs all showed a reduction in synapse number. Increasing electrical excitability, however, only impacted ORN synapse number, while PNs and LNs were unaffected. In the *Drosophila* olfactory system, neuronal activity can influence activity of GSK-3 β (Chiang et al., 2009), a master kinase that promotes cell survival and wiring (the combined processes of axon path-finding and partner matching that result in the correct identification of postsynaptic targets by presynaptic partners), although it is not known how this influences the later developmental step of synaptogenesis, when a functional connection between presynaptic and postsynaptic partners is formed. We found that reducing GSK-3 β kinase activity in ORNs impairs synapse addition, but similar GSK-3 β impairments in PNs and LNs have no effect on synapse formation. Enhancing GSK-3 β activity in both ORNs and LNs, however, phenocopied the effects of reduced neuronal excitability, suggesting that

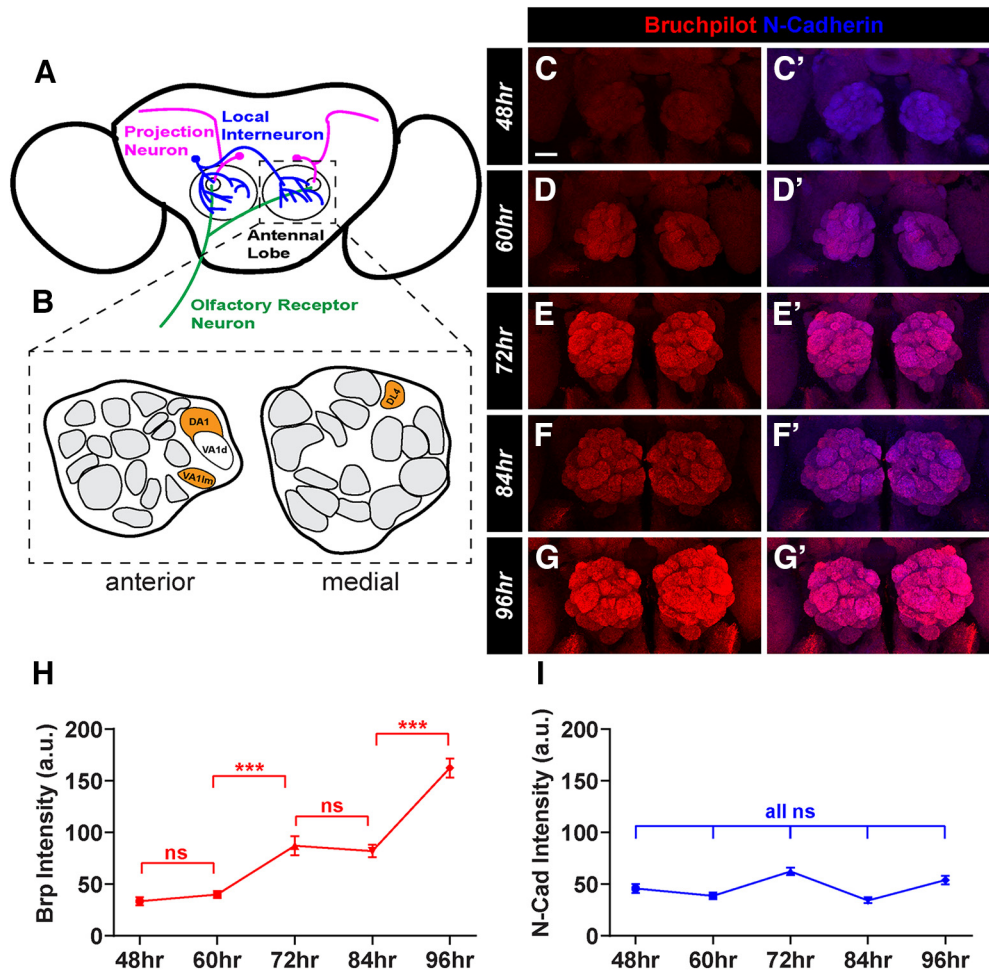


Figure 1. Synapse addition across the antennal lobe during pupal development occurs during distinct time frames. **A, B**, Schematic of the *Drosophila* antennal lobes. Three major neuron classes project to the antennal lobes to relay and process olfactory information: olfactory receptor neurons (green), projection neurons (magenta), and local interneurons (blue; **A**). Each antennal lobe consists of ~50 glomeruli (**B**) with the three glomeruli examined throughout this study (DA1, VA1m, and DL4) highlighted (orange). **C–G'**, Representative confocal image stacks of pupal antennal lobes stained with antibodies to Bruchpilot (red) and N-cadherin (blue) at 48 h (**C**), 60 h (**D**), 72 h (**E**), 84 h (**F**), and 96 h (**G**) after puparium formation. **H, I**, Quantification of average staining intensity for Brp (**H**) and N-cadherin (**I**) from 48 to 96 h APF. Brp intensity increases significantly from 60 to 72 h APF as well as from 84 to 96 h APF. N-cadherin intensity does not change throughout this time frame. For each time point, $n \geq 9$ antennal lobes from 8 brains. $***p < 0.001$. ns = not significant. Scale bar = 20 μm .

electrical activity may function through GSK-3 β to regulate synapse formation. This suggests that although normal activity is required in all three AL neuron classes for mature synaptic development, each class may use different downstream molecular pathways under different circumstances to achieve proper development. These findings demonstrate that, even within the same sensory circuit, synaptic development is not a uniform process for all types of neurons and that the temporal and molecular programs that govern development can vary. Our results reveal novel insights into the mechanisms of synaptic development and demonstrate developmental individuality among different neuron classes.

Materials and Methods

Drosophila stocks and transgenic lines

All control lines and genetic fly stocks were maintained on cornmeal: dextrose medium (Archon Scientific) at 21°C while crosses were raised on similar medium at 25°C (unless noted in the text) in incubators (Darwin Chambers) at 60% relative humidity with a 12/12 h light/dark cycle. Transgenes were maintained over balancers with fluorescent markers and visible phenotypic traits to allow for selection of pupae or adults of the desired genotype. To drive expression in specific classes of antennal lobe neurons, we used the following GAL4 lines: *AM29-GAL4*

(Endo et al., 2007), *Or47b-GAL4* (Vosshall et al., 2000), *Or67d-GAL4* (Stockinger et al., 2005), *Mz19-GAL4* (Jefferis et al., 2004), and *NP3056-GAL4* (Chou et al., 2010). The following UAS transgenes were used as synaptic labels or to express molecular constructs for genetic perturbation experiments: *UAS-Brp-Short-mStraw* (Fouquet et al., 2009; Mosca and Luo, 2014), *UAS-Brp-Short-GFP* (Schmid et al., 2008), *UAS-RBP-GFP* (Liu et al., 2011), *UAS-mCD8-GFP* (Lee and Luo, 1999), *UAS-3xHA-mtdTomato* (Potter et al., 2010), *UAS-NaChBac* (Nitabach et al., 2006), *2xUAS-EKO* (White et al., 2001), *UAS-Sgg-DN* (Franco et al., 2004), *UAS-Sgg-CA* (Bourouis, 2002), *UAS-TNT* (Sweeney et al., 1995), and *UAS-TNT-Imp* (Sweeney et al., 1995). It is important to note that we observe decreased expression of *UAS-mCD8-GFP* in late adulthood when driven by *AM29-GAL4*. However, this decline is not observed when using any other GAL4 line or UAS transgene.

Immunocytochemistry

For time course experiments, male and female pupal brains were dissected at 48, 60, 72, 84, and 92 h after puparium formation (APF) and adult brains were dissected at 0, 3, 6, 9, 12, 15, 18, 21, and 24 d after eclosion. To collect pupae at 0 h APF, white prepupae were selected from vials based on genotype using fluorescent balancer markers and aged to the desired time point. For adults, flies were cleared from vials 1 d before collection and on the following day, newly eclosed adults were chosen based on genotype using identifiable balancers and phenotypic markers.

Flies were then aged to the desired time point before dissection and immunostaining. For experiments involving genetic manipulation of either neuronal or kinase activity, adult brains were dissected at 10 d after eclosion. Brains were fixed in 4% paraformaldehyde for 20 min before being washed in phosphate buffer (1× PB) with 0.3% Triton X-100 (PBT). Brains were then blocked for 1 h in PBT containing 5% normal goat serum (NGS) before being incubated in primary antibodies diluted in PBT with 5% NGS for 2 d at 4°C. Following staining, primary antibodies were discarded and the brains washed 3× 20 min with PBT and incubated in secondary antibodies diluted in PBT with 5% NGS for an additional 2 d at 4°C. The secondary antibodies were then discarded, the brains washed 3× 20 min in PBT, and then incubated overnight in SlowFade (ThermoFisher Scientific) gold antifade mounting media and allowed to sink. Brains were then mounted in SlowFade mounting media using a bridge-mount method with No. 1 cover glass shards and stored at 20°C before being imaged (Wu and Luo, 2006). The following primary antibodies were used: mouse anti-Nc82 (Laissue et al., 1999) rabbit anti-DsRed (TaKaRa Bio, catalog #632496, 1:250; Mosca and Luo, 2014), chicken anti-GFP (Aves, catalog #GFP-1020, 1:1000; Mosca and Luo, 2014), and rat anti-N-cadherin (Hummel and Zipursky, 2004). Alexa568-conjugated (ThermoFisher Scientific) and Alexa647-conjugated (Jackson ImmunoResearch) secondary antibodies were used at 1:250 while FITC-conjugated (Jackson ImmunoResearch) secondary antibodies were used at 1:200. In some cases, nonspecific background recognized by the dsRed antibodies (in the form of large red spots appear around the antennal lobes and outside of the tissue observed). These are part of the background, are not caused by any of the transgenic constructs used (Mosca and Luo, 2014) and did not influence any quantification or scoring methods (see below).

Imaging, analysis, and image processing

All images were obtained using a Zeiss LSM880 Laser Scanning Confocal Microscope (Carl Zeiss) using a 40× 1.4 NA Plan-Apochromat lens or a 63× 1.4 NA Plan-Apochromat f/ELYRA lens at an optical zoom of 3×. Images were centered on the glomerulus of interest and the z-boundaries were set based on the appearance of the synaptic labels, Brp-Short-mStraw and mCD8-GFP. Images were analyzed three dimensionally using the Imaris Software 9.3.1 (Oxford Instruments) on a custom-built image processing computer (Digital Storm) following previously established methods (Mosca and Luo, 2014; Mosca et al., 2017). Both Brp-Short and RBP-GFP puncta were quantified using the “Spots” function with a spot size of 0.6 μm. Neurite volume was quantified using the “Surfaces” function with a local contrast of 3 μm and smoothing of 0.2 μm for *AM29*, *Or47b*, and *Or67d* ORNs or a local contrast of 0.5 and a smoothing of 0.2 μm for *Mz19* PNs and *NP3056* LNs. The resultant masks were then visually inspected to ensure their conformation to immunostaining. Images were processed using ImageJ (NIH) and Adobe Photoshop 2020 (Adobe Systems). Figures were produced using Adobe Illustrator CC 2019 (Adobe Systems).

Statistical analysis

All data were analyzed using Prism 8 (GraphPad Software). This software was also used to generate graphical representations of data. Unpaired Student's *t* tests were used to determine significance between two groups while one-way ANOVA with Tukey's multiple comparisons tests were used to determine significance between groups of three or more. A *p*-value of 0.05 was set as the threshold for significance in all studies. For experiments involving disruption of neuronal activity or kinase activity, multiple concurrent experiments were performed with experimental genotypes as well as wild-type flies and appropriate controls for each genotype. This approach necessitated the need for one-way ANOVA with Tukey's multiple comparisons tests. For each figure, informative genotypes have been presented along with controls appropriate for each genotype.

Genotypes

See Table 1 for all genotypes.

Results

Antennal lobe synapses are added over two distinct phases of pupal development

In the antennal lobe (AL), ORNs, PNs, and LNs (Fig. 1A) comprise three major neuron types that contribute to the detection and subsequent transfer of olfactory information to higher order brain structures (Vosshall et al., 2000; Jefferis et al., 2001; Tanaka et al., 2009). Different classes of each neuron type project to the roughly 50 glomeruli that make up the AL, which are subdivided based on the type of olfactory information they receive (Fig. 1B), and form synapses with each other to generate functional circuits (Suh et al., 2004; Hallem and Carlson, 2006; Jefferis et al., 2007; Grabe and Sachse, 2018). To begin to understand how synapse number changes over time in the antennal lobe at large, we measured the levels of Bruchpilot, an active zone protein and presynaptic marker (Wagh et al., 2006; Fouquet et al., 2009), during pupal development. During the roughly 4-d metamorphic process of pupal development, larvae break down their cellular architecture, including their current nervous system, and reform as an adult fly (Thummel, 2001). Neuronal wiring, axon pathfinding, and partner matching are largely complete by 48 h after puparium formation (APF), indicating that synapses are unlikely to form before the component neurons of the AL have reached their final destination (Komiyama and Luo, 2006). We used antibody staining to measure Bruchpilot intensity (Laissue et al., 1999) from 48 to 96 h APF (Fig. 1C–G). After 96 h APF, pupation is complete and the adult fly ecloses. Quantification of Bruchpilot levels can serve as a measurement of the amount of active zone protein present; in cases of synapse development, the levels of Bruchpilot would necessarily increase concomitantly with synapse addition as sites of neurotransmitter release grow more numerous. Changes in Bruchpilot are consistent with synapse formation and are regulated by genetic and molecular pathways that influence synaptic development (Wagh et al., 2006; Fouquet et al., 2009; Mosca and Luo, 2014; Mosca et al., 2017). We found that average Bruchpilot intensity in the AL increases significantly from 60 to 72 h APF as well as from 84 to 96 h APF (Fig. 1H). Bruchpilot intensity remains largely unchanged, however, between 72 and 84 h APF, suggesting that there are multiple phases of general synapse addition (Fig. 1H). In contrast, the average intensity of N-cadherin, which functions as a general neuropil marker in the fly brain (Hummel and Zipursky, 2004), did not change during the course of pupal development (Fig. 1I). This increase in Bruchpilot levels during development suggests that the total number of synaptic connections within the entire antennal lobe circuit increases during specific time frames.

Pheromone-sensing olfactory receptor neurons develop synapses during pupation then remove synapses in late adulthood

Our results suggest that the multiple classes of antennal lobe neurons, when considered together, add synapses during specific time frames of pupal development (Fig. 1). However, our data represents the aggregate of all neuronal classes and does not distinguish between each of the major classes of antennal lobe neurons (ORNs, PNs, and LNs). To understand how the cell-type specific synaptic development of each class of neurons progresses, we expressed Bruchpilot-Short (Brp-Short), an active zone label associated with presynaptic contacts (Mosca and Luo, 2014), in each class of neurons using the UAS-GAL4 binary expression system (Brand and Perrimon, 1993). We performed a high-resolution time course analysis

Table 1. Genotypes for each figure panel

Figure	Panel	Genotype
1	C–G	+; +; +; +
2	B–M	w; Or47b-GAL4 / UAS-Brp-Short-mStraw, UAS-mCD8-GFP; +; +
3	B–K	w; Or47b-GAL4 / UAS-Brp-Short-mStraw, UAS-mCD8-GFP; +; +
4, 5	B–J	w; UAS-Brp-Short-mStraw, UAS-mCD8-GFP / +; Or67d-GAL4 / +; +
6	A–U	w; UAS-Brp-Short-mStraw, UAS-mCD8-GFP / UAS-RBP-GFP; Or67d-GAL4 / +; +
7, 8	B–O	w; AM29-GAL4 / UAS-Brp-Short-mStraw, UAS-mCD8-GFP; +; +
9, 10	B–O	w; Mz19-GAL4 / UAS-Brp-Short-mStraw, UAS-mCD8-GFP; +; +
11, 12	B–O	w; UAS-Brp-Short-mStraw, UAS-mCD8-GFP / +; NP3056-GAL4 / +; +
13, 14	A	w; UAS-Brp-Short-mStraw / UAS-TNT-imp; Or67d-GAL4 / +; +
	B	w; UAS-Brp-Short-mStraw / UAS-TNT; Or67d-GAL4 / +; +
	C	w; UAS-Brp-Short-mStraw / 2×UAS-EKO; Or67d-GAL4 / +; +
	D	w; UAS-mCD8-GFP / UAS-TNT-imp; Or67d-GAL4 / +; +
	E	w; UAS-mCD8-GFP / UAS-TNT; Or67d-GAL4 / +; +
	F	w; UAS-mCD8-GFP / 2×UAS-EKO; Or67d-GAL4 / +; +
	H, K	w; Mz19-GAL4, UAS-3×HA-mtdTomato / UAS-TNT-imp; UAS-Brp-Short-GFP / +; +
	I, L	w; Mz19-GAL4, UAS-3×HA-mtdTomato / UAS-TNT; UAS-Brp-Short-GFP / +; +
	J, M	w; Mz19-GAL4, UAS-3×HA-mtdTomato / 2×UAS-EKO; UAS-Brp-Short-GFP / +; +
	O	w; UAS-Brp-Short-mStraw / UAS-TNT-imp; NP3056-GAL4 / +; +
	P	w; UAS-Brp-Short-mStraw / UAS-TNT; NP3056-GAL4 / +; +
	Q	w; UAS-Brp-Short-mStraw / 2×UAS-EKO; NP3056-GAL4 / +; +
	R	w; UAS-mCD8-GFP / UAS-TNT-imp; NP3056-GAL4 / +; +
	S	w; UAS-mCD8-GFP / UAS-TNT; NP3056-GAL4 / +; +
	T	w; UAS-mCD8-GFP / 2×UAS-EKO; NP3056-GAL4 / +; +
15, 16	A	w; UAS-Brp-Short-mStraw / +; Or67d-GAL4 / +; +
	B	w; UAS-Brp-Short-mStraw / UAS-NaChBac; Or67d-GAL4 / +; +
	C	w; UAS-mCD8-GFP / +; Or67d-GAL4 / +; +
	D	w; UAS-mCD8-GFP / UAS-NaChBac; Or67d-GAL4 / +; +
	F, H	w; Mz19-GAL4, UAS-3×HA-mtdTomato / +; UAS-Brp-Short-GFP / +; +
	G, I	w; Mz19-GAL4, UAS-3×HA-mtdTomato / UAS-NaChBac; UAS-Brp-Short-GFP / +; +
	K	w; UAS-Brp-Short-mStraw / +; NP3056-GAL4 / +; +
	L	w; UAS-Brp-Short-mStraw / UAS-NaChBac; NP3056-GAL4 / +; +
	M	w; UAS-mCD8-GFP / +; NP3056-GAL4 / +; +
	N	w; UAS-mCD8-GFP / UAS-NaChBac; NP3056-GAL4 / +; +
17, 18	A	w; UAS-Brp-Short-mStraw / +; Or67d-GAL4 / +; +
	B	w; UAS-Brp-Short-mStraw / UAS-Sgg-CA; Or67d-GAL4 / +; +
	C	w; UAS-mCD8-GFP / +; Or67d-GAL4 / +; +
	D	w; UAS-mCD8-GFP / UAS-Sgg-CA; Or67d-GAL4 / +; +
	F	w; UAS-Brp-Short-mStraw / +; NP3056-GAL4 / +; +
	G	w; UAS-Brp-Short-mStraw / UAS-Sgg-CA; NP3056-GAL4 / +; +
	H	w; UAS-mCD8-GFP / +; NP3056-GAL4 / +; +
	I	w; UAS-mCD8-GFP / UAS-Sgg-CA; NP3056-GAL4 / +; +
19, 20	A	w; UAS-Brp-Short-mStraw / +; Or67d-GAL4 / +; +
	B	w; UAS-Brp-Short-mStraw / UAS-Sgg-DN; Or67d-GAL4 / +; +
	C	w; UAS-mCD8-GFP / +; Or67d-GAL4 / +; +
	D	w; UAS-mCD8-GFP / UAS-Sgg-DN; Or67d-GAL4 / +; +
	F, H	w; Mz19-GAL4, UAS-3×HA-mtdTomato / +; UAS-Brp-Short-GFP / +; +
	G, I	w; Mz19-GAL4, UAS-3×HA-mtdTomato / UAS-Sgg-DN; UAS-Brp-Short-GFP / +; +
	K	w; UAS-Brp-Short-mStraw / +; NP3056-GAL4 / +; +
	L	w; UAS-Brp-Short-mStraw / UAS-Sgg-DN; NP3056-GAL4 / +; +
	M	w; UAS-mCD8-GFP / +; NP3056-GAL4 / +; +
	N	w; UAS-mCD8-GFP / UAS-Sgg-DN; NP3056-GAL4 / +; +

of synaptic development throughout pupation and adulthood using confocal microscopy followed by three-dimensional rendering (see Materials and Methods). Brp-Short is a fluorescently tagged truncated variant of the active zone protein Bruchpilot (Fouquet et al., 2009; Mosca and Luo, 2014) that interacts with full-length Bruchpilot without interfering with its function or adding ectopic synapses (Wagh et al., 2006; Fouquet et al., 2009; Mosca and Luo, 2014; Mosca et al., 2017). Brp-Short signal manifests as synaptically localized puncta, acting as a proxy label for active zones, and accurately reports synapse number from specific cell populations and fold changes in synapse number because of genetic

perturbation, as supported by genetic and electron microscopy studies (Fouquet et al., 2009; Kremer et al., 2010; Christiansen et al., 2011; Berger-Müller et al., 2013; Mosca and Luo, 2014; Coates et al., 2017, 2020; Mosca et al., 2017). We also labeled each neuronal class examined with membrane-bound GFP to fluorescently label neurites (Lee and Luo, 1999), enabling the quantification of neurite volume for each neuron class within a given glomerulus (Mosca and Luo, 2014; Mosca et al., 2017). To establish a time course of synaptic development, we quantified Brp-Short puncta and neuronal membrane volume marked by mCD8-GFP every 12 h from 48 to 92 h APF and then every 3–5 d, at regular

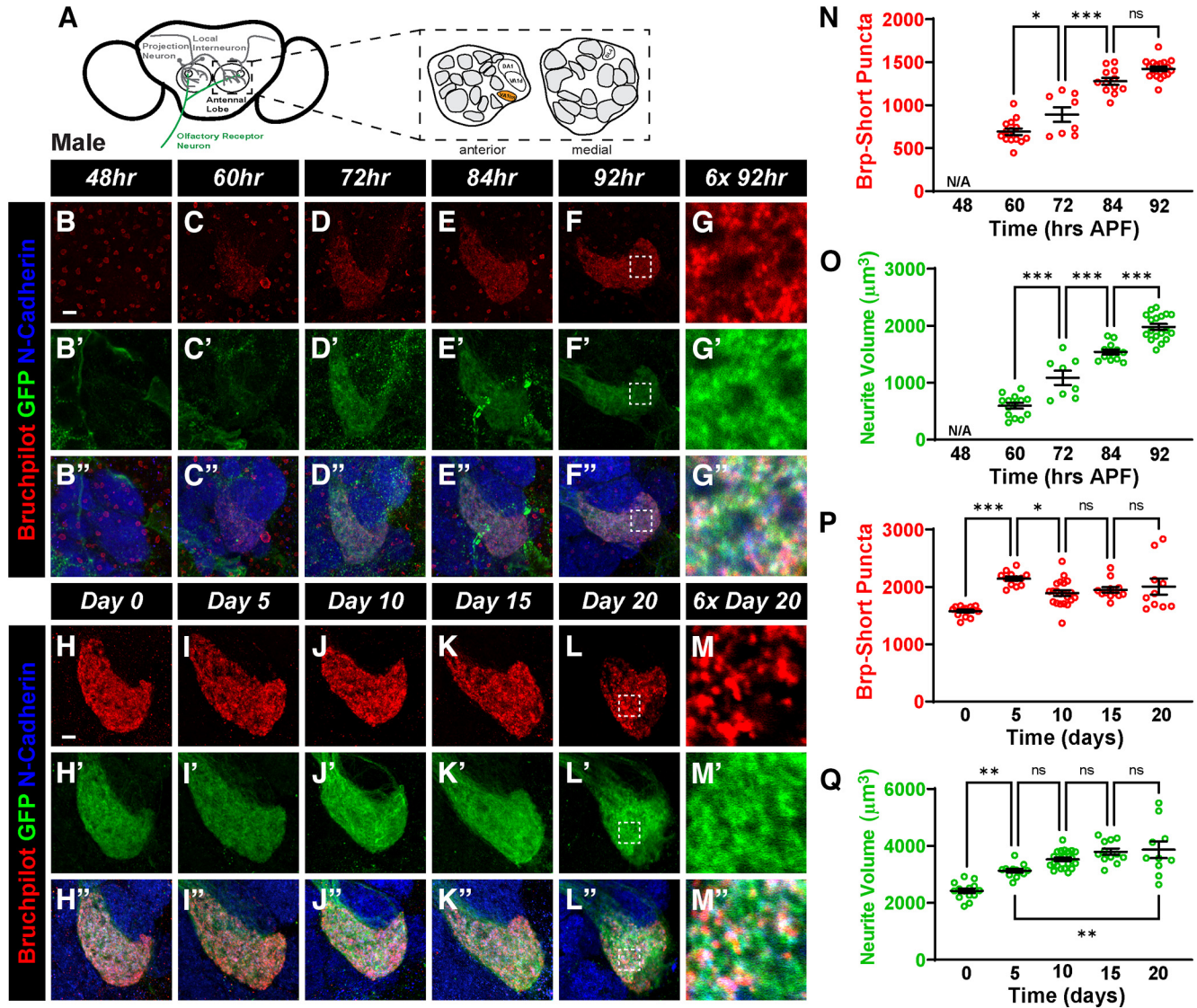


Figure 2. A developmental time course of synapse number and neurite volume in male VA1Im ORNs. **A**, Schematic of the *Drosophila* antenna lobes showing ORNs (green) of the VA1Im glomerulus (orange). **B–F'**, Representative confocal image stacks of male pupal VA1Im ORNs expressing Brp-Short-mStraw and membrane-tagged GFP and stained with antibodies against mStraw (red), GFP (green), and N-cadherin (blue) at 48 h (**B**), 60 h (**C**), 72 h (**D**), 84 h (**E**), and 92 h (**F**) APF. **G–G'**, High-magnification, single optical section of ORNs aged to 92 h APF from inset in **F** showing synaptic labels. Note that synaptic puncta are not evident until 60 h APF. **H–L'**, Representative confocal image stacks of male adult VA1Im ORNs expressing Brp-Short-mStraw and membrane-tagged GFP and stained with antibodies as in **B–F'** at 0 d (**H**), 5 d (**I**), 10 d (**J**), 15 d (**K**), and 20 d (**L**) after eclosion. **M–M'**, High-magnification, single optical section of 20-d-old ORNs from inset in **L** showing synaptic labels. **N, O**, Quantification of Brp-Short-mStraw puncta (**N**) and membrane GFP volume (**O**) for pupal male ORNs. Both synaptic puncta and neurites are not measurable until 60 h APF, at which point they increase during the remainder of pupal development. **P, Q**, Quantification of Brp-Short-mStraw puncta (**P**) and membrane GFP (**Q**) volume for adult male ORNs. Synaptic puncta significantly increase from 0 to 5 d old and then decrease between 5 and 10 d after eclosion. Neurite volume increases from 0 to 15 d of age before achieving a steady state. For each time point, $n \geq 8$ glomeruli from 4 brains. * $p < 0.05$, ** $p < 0.01$, *** $p < 0.001$, ns = not significant. Scale bar = 5 μm . Raw data are provided in Extended Data Table 2-1.

intervals, from 0 to 24 d after eclosion in ORN classes that innervate distinct glomeruli. We specifically assayed pupal synapse development at 92 h APF to ensure that all pupae were collected before eclosion (at 25°C, adult eclosion typically occurs between 92 and 96 h APF).

ORNs are the primary sensory neurons responsible for conveying odorant information from the environment to the antenna lobes (Wilson, 2013). We first sought to assess the temporal synaptic development of ORNs that project to the VA1Im glomerulus (Fig. 2A) and are genetically accessed by *Or47b-GAL4* (Vosshall et al., 2000). This glomerulus receives pheromone odorant information (Vosshall et al., 2000; Fishilevich and Vosshall, 2005), is involved in oviposition as well as courtship decisions, influencing preference for younger mates (Zhuang et

al., 2016; Chin et al., 2018; Sethi et al., 2019), and is sexually dimorphic, with male glomeruli being ~40% larger than female glomeruli (Fishilevich and Vosshall, 2005; Mosca and Luo, 2014). We quantified Brp-Short puncta and neurite volume at 48, 60, 72, 84, and 92 h APF as well as at 0, 5, 10, 15, and 20 d after eclosion (Fig. 2B–M') in both male and females separately to assay any sexual dimorphisms in synaptic development. In male pupal ORNs, there were no synapses detectable at 48 h APF, but synapses were then steadily added over pupal development with the number of Brp-Short puncta doubling from 60 to 92 h APF (Fig. 2N; Extended Data Table 2-1). Neurite volume was also negligible at 48 h APF, possibly because the neurons must become more mature before mCD8-GFP can stably localize to the membrane, but then increased 3-fold from 60 h APF to 92 h

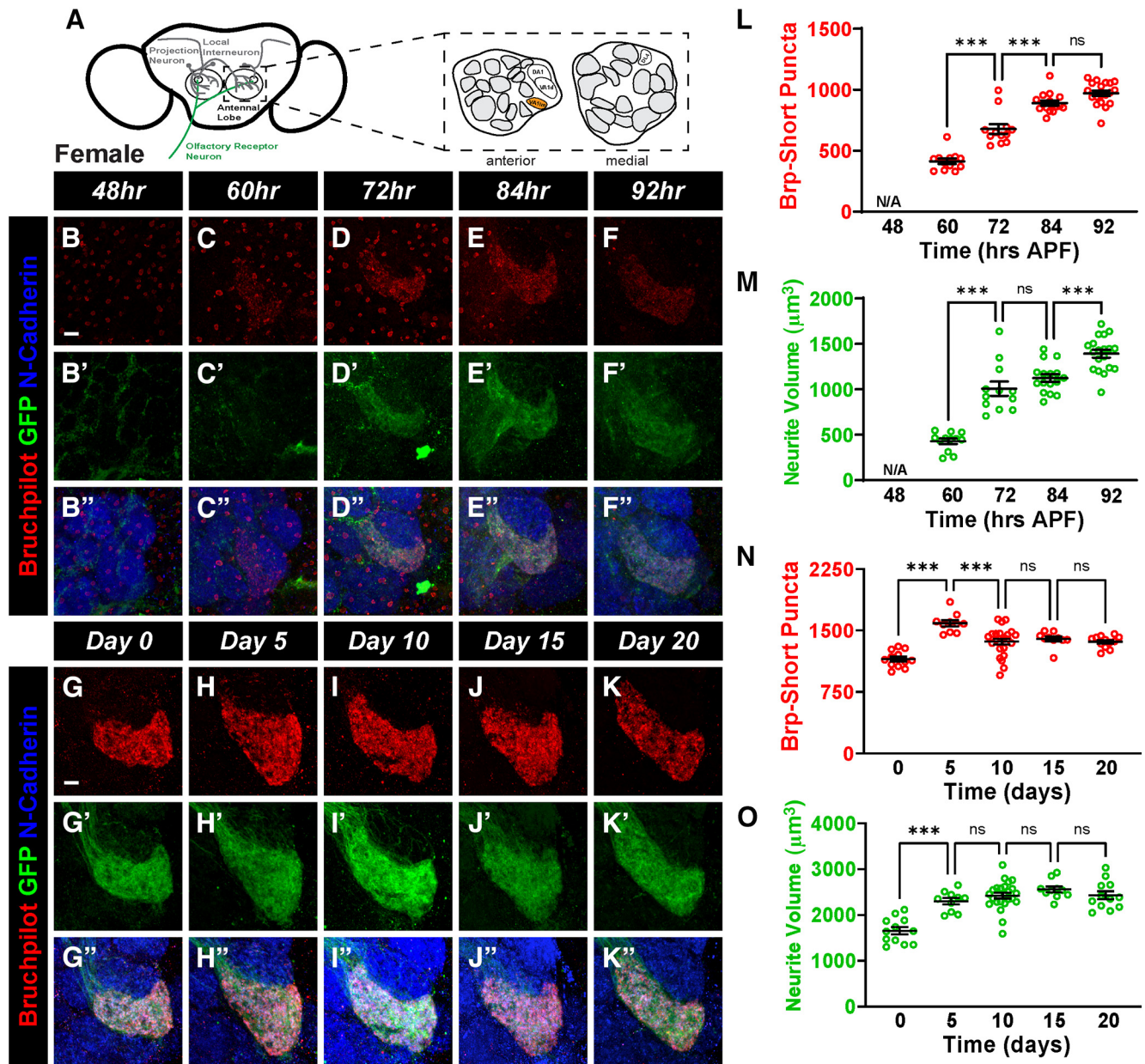


Figure 3. Synapse formation for female ORNs of the VA1Im glomerulus. **A**, Schematic of the *Drosophila* antennal lobes showing ORNs (green) of the VA1Im glomerulus (orange). **B–F''**, Representative confocal image stacks of female pupal VA1Im ORNs expressing Brp-Short-mStraw and membrane-tagged GFP and stained with antibodies against mStraw (red), GFP (green), and N-cadherin (blue) at 48 h (**B**), 60 h (**C**), 72 h (**D**), 84 h (**E**), and 92 h (**F**) APF. Note that synaptic puncta do not appear until 60 h APF. **G–K''**, Representative confocal image stacks of female adult VA1Im ORNs expressing Brp-Short-mStraw and membrane-tagged GFP and stained with antibodies as in **B–F''** at 0 d (**G**), 5 d (**H**), 10 d (**I**), 15 d (**J**), and 20 d (**K**) after eclosion. **L, M**, Quantification of Brp-Short-mStraw puncta (**L**) and membrane GFP volume (**M**) for pupal female ORNs. Both synaptic puncta and neurites are not measurable until 60 h APF, at which point they increase during the remainder of pupal development. **N, O**, Quantification of Brp-Short-mStraw puncta (**N**) and membrane GFP (**O**) volume for adult female ORNs. Synaptic puncta significantly increase from 0 to 5 d old and then decrease between 5 and 10 d after eclosion. Neurite volume increases from 0 to 5 d of age before achieving a steady state. For each time point, $n \geq 10$ glomeruli from 5 brains. *** $p < 0.001$, ns = not significant. Scale bar = 5 μm . Raw data are provided in Extended Data Table 3-1.

APF (Fig. 2O; Extended Data Table 2-1). This glomerulus-specific time course of synapse formation differs from the time course of gross AL synapse formation (Fig. 1) in that synapses were added steadily throughout pupal development rather than in two separated time periods. After eclosion, there was a 36% increase in the number of Brp-Short puncta from 0 to 5 d of age followed by a 13% decrease in puncta number from 5 to 10 d of age (Fig. 2P; Extended Data Table 2-1). Following 10 d of age, synapse number remained constant throughout the analysis. Adult neurite volume increased by 29% between 0 and 5 d after eclosion and then an additional 21% by 15 d after eclosion (Fig.

2Q; Extended Data Table 2-1). Together, these data suggest that synapses are steadily added from 48 h APF to 5 d after eclosion, demonstrating that individual classes of olfactory neurons may show distinct synapse addition phases than the aggregate antennal lobe. This is followed by a pruning phase where synapses are removed before the completion of synaptic development and establishment of a steady state synapse number. Neurites continually grow and add volume until 15 d after eclosion, after which point, they achieve a steady state volume. We additionally determined the time course of female VA1Im ORN synaptic development (Fig. 3A–K'') to determine whether any of the

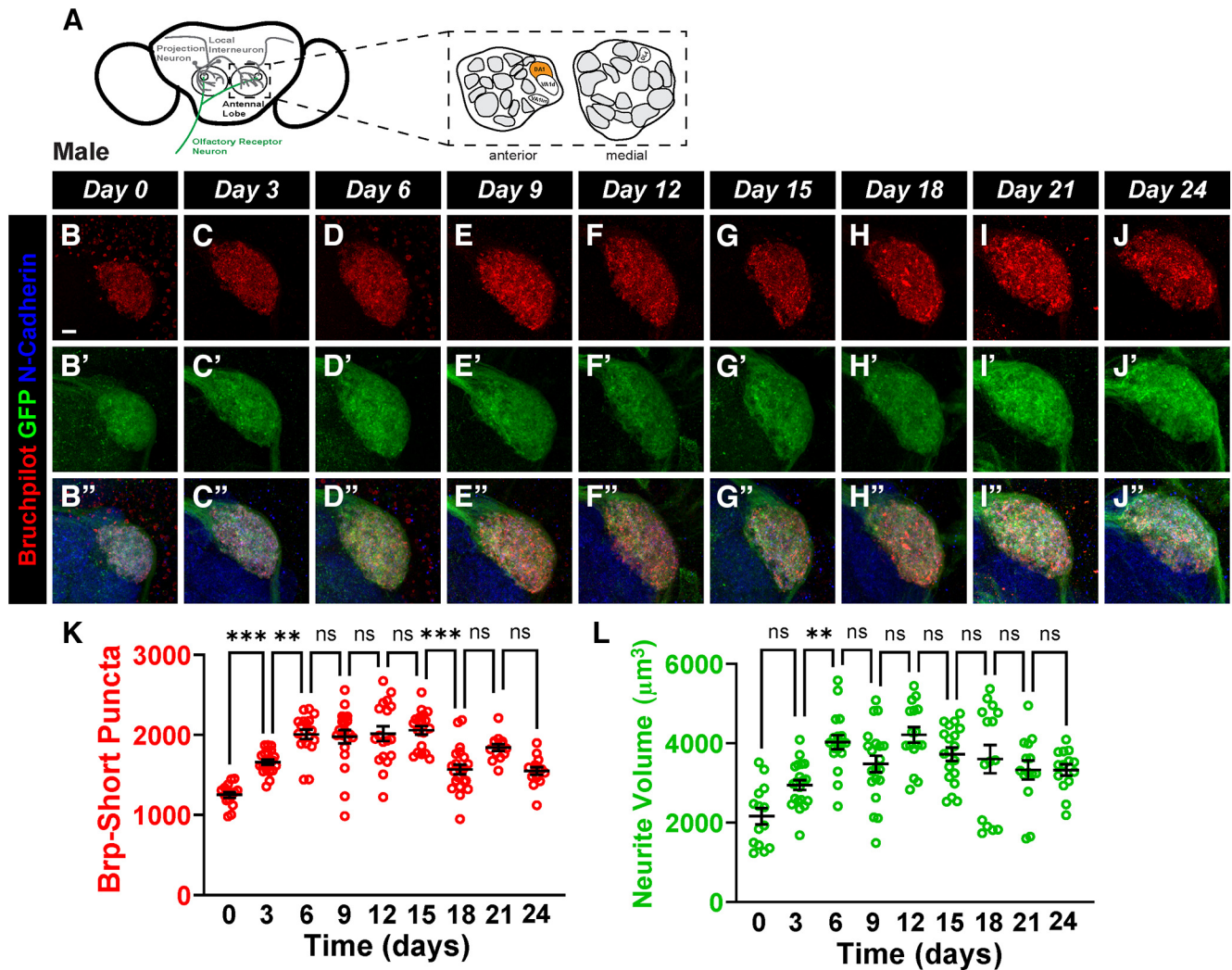


Figure 4. A developmental time course of synapse number and neurite volume in adult male DA1 ORNs. **A**, Schematic of the antennal lobes showing ORNs (green) of the DA1 glomerulus (orange). **B–J''**, Representative confocal image stacks of male adult DA1 ORNs expressing Brp-Short-mStraw and membrane-tagged GFP and stained with antibodies against mStraw (red), GFP (green), and N-cadherin (blue) at 0 d (**B**), 3 d (**C**), 6 d (**D**), 9 d (**E**), 12 d (**F**), 15 d (**G**), 18 d (**H**), 21 d (**I**), and 24 d (**J**) of age. **K**, **L**, Quantification of Brp-Short-mStraw puncta (**K**) and membrane GFP volume (**L**) for adult male DA1 ORNs. Both Brp-Short puncta number and neurite volume steadily increase from 0 to 6 d of age; after 6 d after eclosion, neurite volume stabilizes while Brp-Short puncta maintain a steady state before decreasing between 15 and 18 d of age. For each time point, $n \geq 14$ glomeruli from 7 brains. ** $p < 0.01$, *** $p < 0.001$, ns = not significant. Scale bar = $5 \mu\text{m}$. Raw data are provided in Extended Data Table 4-1.

developmental mechanisms displayed sexual dimorphism or whether they occurred similarly to male ORNs. There were fewer Brp-Short puncta and lower neurite volume at all time points in female VA11m ORNs compared with male VA11m ORNs, consistent with established sexual dimorphisms in size and synapse number (Stockinger et al., 2005; Mosca and Luo, 2014). We found that females also had a 2-fold increase in puncta and 3-fold increase in neurite volume from 60 to 92 h APF (Fig. 3L,M; Extended Data Table 3-1). Adult female ORNs exhibited a similar increase in Brp-Short puncta to the male ORNs from 0 to 5 d of age that was followed by a decrease from 5 to 10 d after eclosion (Fig. 3N; Extended Data Table 3-1). Adult neurite volume, however, significantly increased from 0 to 5 d after eclosion and then did not significantly change afterward (Fig. 3O; Extended Data Table 3-1), suggesting that female ORNs achieve their mature adult volume earlier than male ORNs. This suggests similarities in the general addition of synapses throughout development despite sexual dimorphisms in absolute synapse number but a minor difference in the growth rate of neurites during development between males

and females. Overall, these time courses demonstrate a general, previously unappreciated, pattern of synaptic development for a sexually-dimorphic, pheromone-specific glomerulus in which synapses continually form until 5 d after eclosion and then decrease before stabilizing to a mature quantity.

We next sought to determine whether another sexually dimorphic class of ORNs, the Or67d-positive ORNs that project to the DA1 glomerulus (Fig. 4A), develop similarly to VA11m ORNs or whether there are differences based on glomerulus (Datta et al., 2008). DA1 ORNs detect male pheromones, including 11-*cis*-Vaccenyl acetate, that are involved in courtship and aggression for both male and female flies (Kurtovic et al., 2007; Datta et al., 2008; Wilson, 2013). Similar to VA11m, DA1 is a sexually-dimorphic glomerulus with increased glomerular size in males compared with females (Stockinger et al., 2005; Mosca and Luo, 2014). We used a GAL4 driver that labels DA1 ORNs via GAL4 expression under the control of the endogenous *Or67d* promoter (Stockinger et al., 2005) to examine the time course of synapse formation during adult stages; *Or67d-GAL4* is not active during pupal development precluding our analysis of synapse

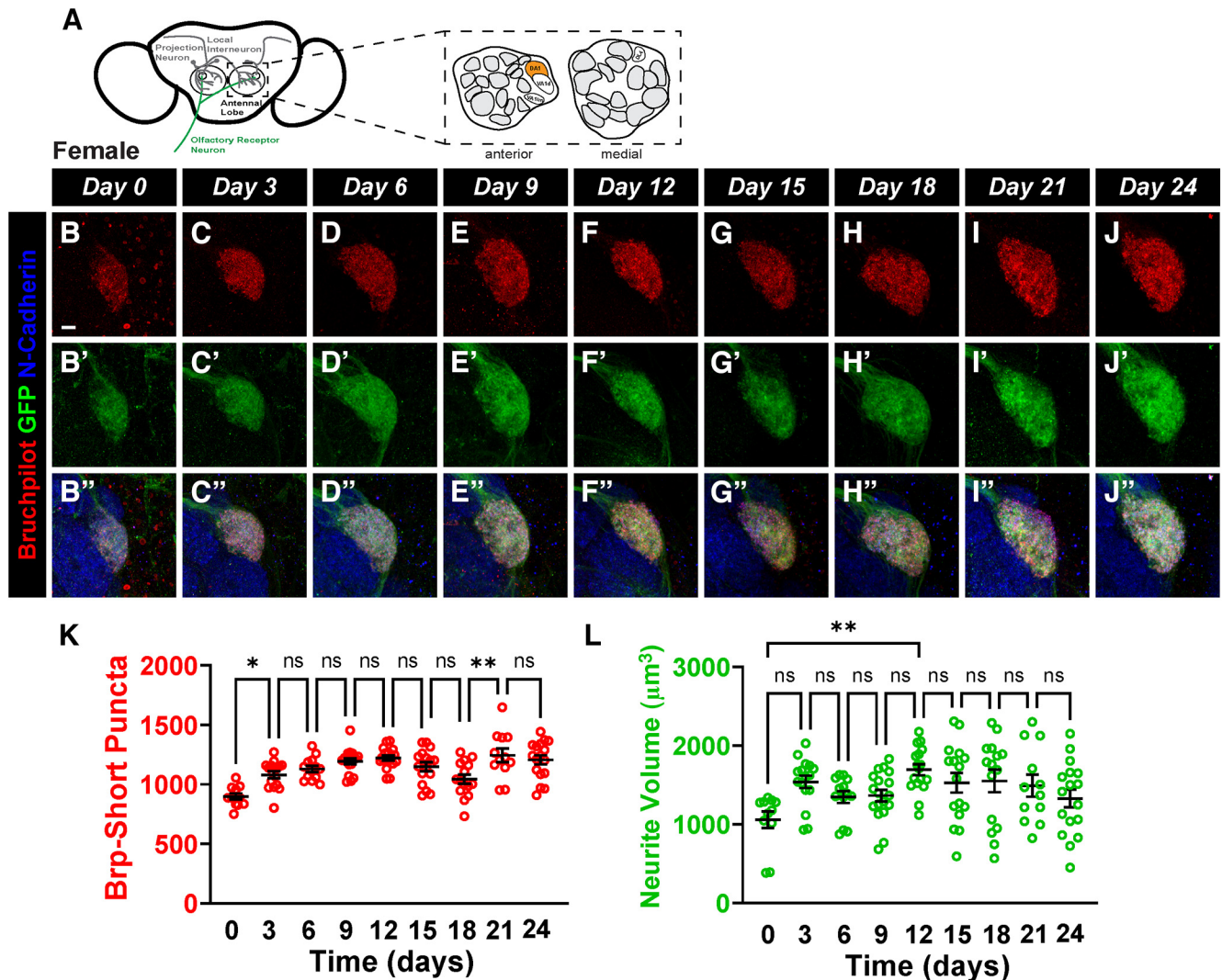


Figure 5. Synapse formation for the DA1 glomerulus in female ORNs. *A*, Schematic of the antennal lobes showing ORNs (green) of the DA1 glomerulus (orange). *B–J'*, Representative confocal image stacks of female adult DA1 ORNs expressing Brp-Short-mStraw and membrane-tagged GFP and stained with antibodies against mStraw (red), GFP (green), and N-cadherin (blue) at 0 (*B*), 3 (*C*), 6 d (*D*), 9 d (*E*), 12 d (*F*), 15 d (*G*), 18 d (*H*), 21 d (*I*), and 24 d (*J*) of age. *K*, *L*, Quantification of Brp-Short-mStraw puncta (*K*) and membrane GFP volume (*L*) for adult female DA1 ORNs. Both Brp-Short puncta number and neurite volume steadily increase from 0 to 3 d of age, after which neurite volume stabilizes. Brp-Short puncta maintain a steady state before decreasing and subsequently increasing between 15 and 21 d of age. For each time point, $n \geq 11$ glomeruli from 6 brains. * $p < 0.05$, ** $p < 0.01$, ns = not significant. Scale bar = 5 μm . Raw data are provided in Extended Data Table 5-1.

development in these ORNs from 48 to 92 h APF. We quantified Brp-Short puncta number and neurite volume for male DA1 ORNs every 3 d from 0 to 24 d of age (Fig. 4*B–J'*) and found that Brp-Short puncta increased by 50% between 0 and 6 d of age before achieving and maintaining a steady state synapse number until day 15. Surprisingly, we observed a 25% decline in synapse number between days 15 and 18 (Fig. 4*K*; Extended Data Table 4-1). Neurite volume doubled from 0 to 6 d old and then did not significantly change for the remainder of adulthood (Fig. 4*L*; Extended Data Table 4-1), thus maintaining a steady state. We found congruent results with female DA1 ORNs (Fig. 5*A–J'*). Brp-Short puncta number in female ORNs significantly increased by 20% (Fig. 5*K*; Extended Data Table 5-1) from 0 to 3 d of age, maintained a steady state from 3 to 12 d, and then trended down by 15% from 12 to 18 d of age. Puncta number then significantly increased by 19% from 18 to 21 d of age before stabilizing for the remainder of adulthood. Neurite volume significantly increased by 60% from 0 to 12 d of age and then did not significantly change for the rest of adulthood (Fig. 5*L*;

Extended Data Table 5-1). Thus, the general female time course of DA1 ORNs was nearly identical to the male time course, with slight variability in the exact times of synapse change. Compared with VA11m ORNs, DA1 ORN synapse development showed similar synapse addition until 5–6 d after eclosion but did not display a synapse reduction phase until 12–18 d old, while VA11m ORNs displayed synapse pruning from 5–10 d old. These data imply that pheromone-specific ORNs follow similar general patterns of synaptic development but have critical differences in the exact timing of developmental phases.

Bruchpilot represents a core component of the active zone and is an accurate reporter of synaptic release sites (Kittel et al., 2006; Wagh et al., 2006; Mosca and Luo, 2014). However, Bruchpilot protein levels can show changes that are independent of changes in synapse number (Sugie et al., 2015; Woźnicka et al., 2015). Therefore, we also sought to examine the time course of DA1 ORN synaptic development using an additional synapse marker that was independent of Brp-Short to ensure that the differences we observed were reflective of synaptic connections and

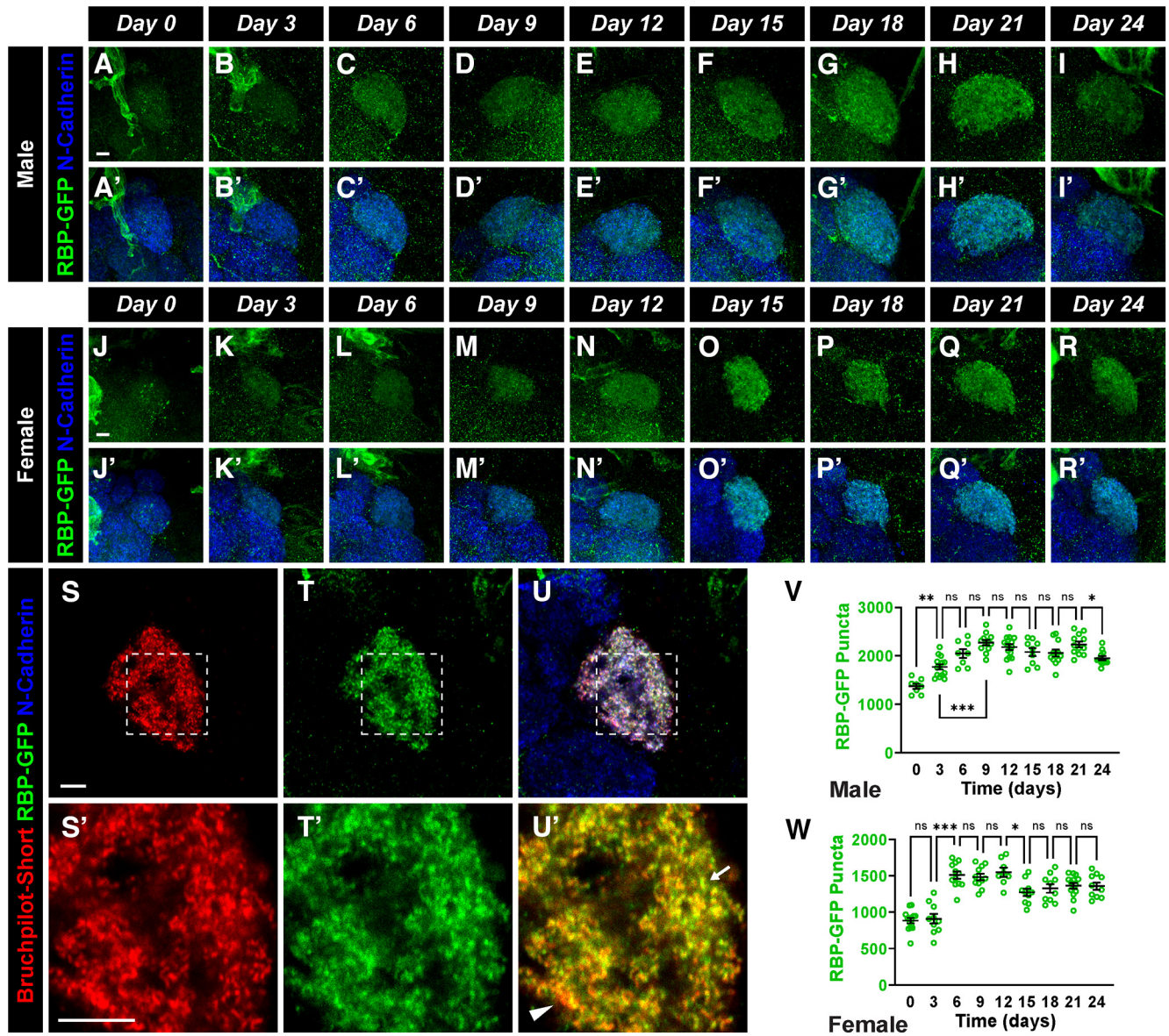


Figure 6. Developmental time courses of synapse formation using RIM-Binding Protein in male and female DA1 ORNs. *A–I'*, Representative confocal image stacks of male adult DA1 ORNs expressing RIM-Binding Protein-tagged GFP (RBP-GFP) and stained with antibodies against GFP (green) and N-cadherin (blue) at 0 d (*A*), 3 d (*B*), 6 d (*C*), 9 d (*D*), 12 d (*E*), 15 d (*F*), 18 d (*G*), 21 d (*H*), and 24 d (*I*) of age. *J–R'*, Representative confocal image stacks of female adult DA1 ORNs expressing RBP-GFP and stained with antibodies as in *A–I'* at 0 d (*J*), 3 d (*K*), 6 d (*L*), 9 d (*M*), 12 d (*N*), 15 d (*O*), 18 d (*P*), 21 d (*Q*), and 24 d (*R*) of age. *S–U'*, Single optical sections with high-magnification insets (dashed boxes) of female DA1 ORNs at 24 d of age expressing Brp-Short-mStraw and RBP-GFP and stained with antibodies against mStraw (red), GFP (green), and N-cadherin (blue). *V*, Quantification of RBP-GFP puncta for male DA1 ORNs. RBP-GFP puncta number increases until between 6 and 9 d of age. RBP-GFP puncta maintain a steady-state until decreasing at 24 d of age. *W*, Quantification of RBP-GFP puncta for female DA1 ORNs. RBP-GFP puncta number increases until 6 d of age. RBP-Puncta maintain a steady-state until puncta number decreases at 15 d of age, stabilizing for the remainder of adulthood. For each time point, $n \geq 8$ glomeruli from 6 brains. * $p < 0.05$, ** $p < 0.01$, *** $p < 0.001$, ns = not significant. Scale bar = 5 μm .

not simply changes in the Bruchpilot protein itself. The presynaptic active zone is comprised of multiple proteins that function together to recruit and release synaptic vesicles during neurotransmission (Südhof, 2012). RIM-BP, the Rab3-interacting molecule (RIM)-binding protein, is an essential active zone protein that couples synaptic vesicle recruitment machinery to vesicle release architecture (Hibino et al., 2002; Kiss et al., 2011; Petzoldt et al., 2020). In *Drosophila*, RIM-BP is a central component of the active zone (Liu et al., 2011) and labels most, if not all active zones in the fly nervous system. To examine the time course of synaptic development, we expressed a GFP-tagged transgenic RIM-BP (RBP-GFP) using *Or67d-GAL4* and quantified RBP-GFP puncta from 0 to 24 d of age for both males (Fig. 6*A–I'*) and females (Fig. 6*J–R'*) in a fashion analogous to our Brp-Short

experiments. When co-expressed in the same *Or67d*-positive ORNs, we observed near (but not complete) overlap between Brp-Short and RBP-GFP puncta (Fig. 6*S–U'*), suggesting that they were both labeling a nearly identical population of synaptic contacts. In male ORNs, we found that RBP-GFP puncta significantly increased by 66% (Fig. 6*V*) from 0 to 9 d of age and then maintained a steady-state throughout most of adulthood. RBP-GFP puncta then significantly decreased by 13% from 21 to 24 d of age. For female ORNs, RBP-GFP puncta number significantly increased by 66% (Fig. 6*W*) from 3 to 6 d of age before maintaining a steady-state for much of adulthood. Similarly to the male ORNs, RBP-GFP puncta significantly decreased by 18% between 12 and 15 d of age before stabilizing for the remainder of observed adulthood. Just as we found with the Brp-Short time

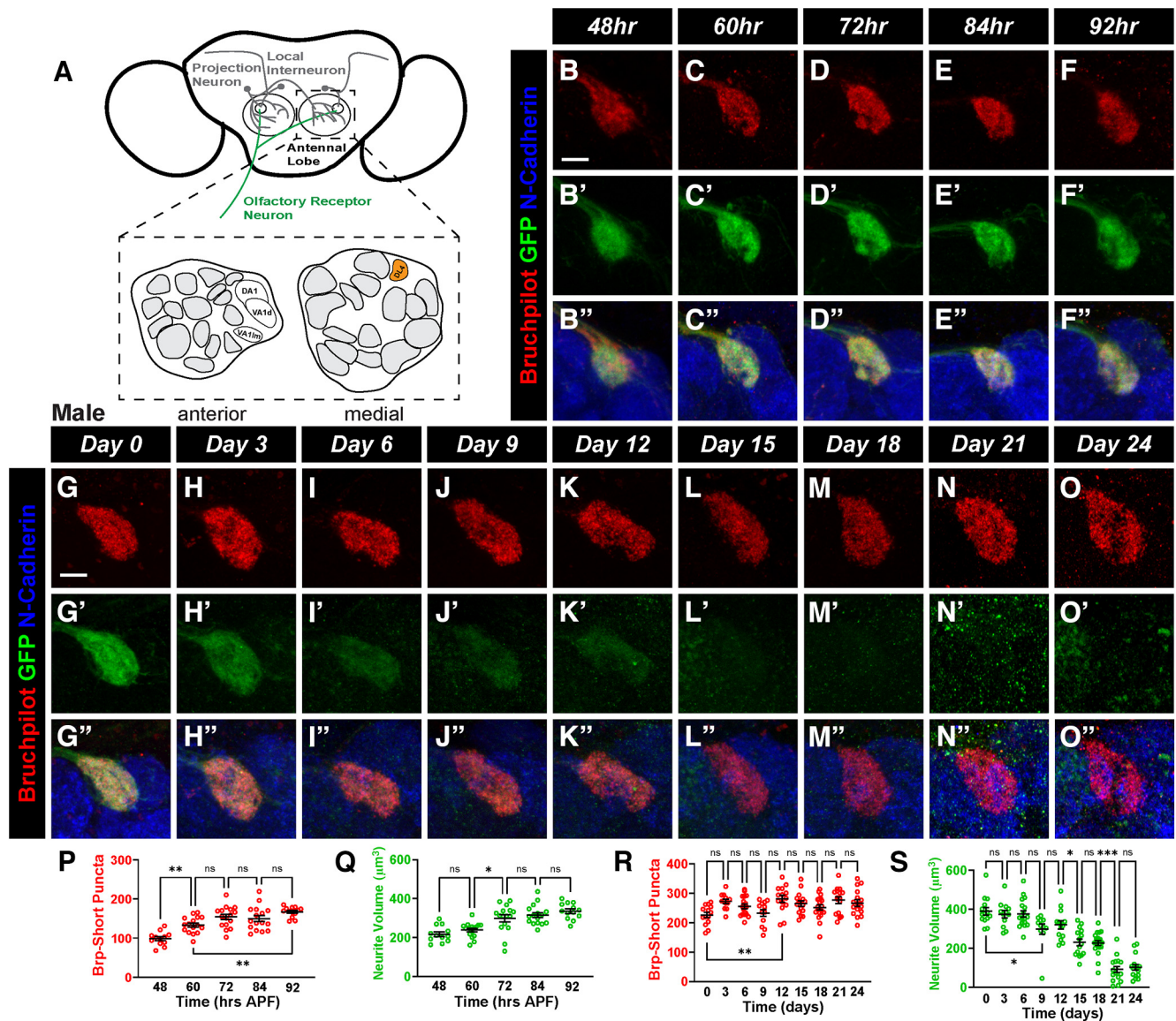


Figure 7. A developmental time course of synapse number and neurite volume in male DL4 ORNs. *A*, Schematic of the *Drosophila* antennal lobes showing ORNs (green) of the DL4 glomerulus (orange). *B–F'*, Representative confocal image stacks of male pupal DL4 ORNs expressing Brp-Short-mStraw and membrane-tagged GFP and stained with antibodies against mStraw (red), GFP (green), and N-cadherin (blue) at 48 h (*B*), 60 h (*C*), 72 h (*D*), 84 h (*E*), and 92 h (*F*) APF. *G–O'*, Representative confocal image stacks of male adult DL4 ORNs expressing Brp-Short-mStraw and membrane-tagged GFP and stained with antibodies as in *B–F'* at 0 d (*G*), 3 d (*H*), 6 d (*I*), 9 d (*J*), 12 d (*K*), 15 d (*L*), 18 d (*M*), 21 d (*N*), and 24 d (*O*) of age. *P, Q*, Quantification of Brp-Short-mStraw puncta (*P*) and membrane GFP volume (*Q*) for pupal male DL4 ORNs. Both synaptic puncta and neurite volume increase throughout pupal development. *R, S*, Quantification of synaptic puncta (*R*) and neurite volume (*S*) for adult male DL4 ORNs. Synaptic puncta trends upward from 0 to 3 d of age and then stabilize. Neurite volume steadily decreases over time. For each time point, $n \geq 11$ glomeruli from 6 brains. * $p < 0.1$, ** $p < 0.01$, *** $p < 0.001$, ns = not significant. Scale bar = 5 μm . Raw data are provided in Extended Data Table 7-1.

courses of DA1 ORNs (Figs. 4 and 5), the RBP-GFP time courses of synapse formation for males and females were nearly identical with only slight variations in the timings of synapse change. The similarity of the time courses obtained using either Brp-Short or RIM-BP imaging validate that our findings can accurately demonstrate the temporal pattern of synaptic development for ORNs.

Food-sensing olfactory receptor neurons develop synapses during pupation and early adulthood then stabilize

Drosophila rely on olfaction to find and interact with mates as well as identify suitable food sources. Food sensing glomeruli lack sexual dimorphism seen in size and synapse number of pheromone-sensing glomeruli (Couto et al., 2005; Stockinger et al., 2005; Mosca and Luo, 2014), likely because all flies have a

shared, unabating need to identify food sources. Our assays on sexually dimorphic glomeruli thus far followed the synaptic development of pheromone-sensing ORNs but we further sought to understand whether the same developmental features apply in glomeruli that sense food odorants or whether these glomeruli followed a distinct developmental program. We first established a time course for male ORNs that project to the DL4 glomerulus (Fig. 7*A*), a class of neurons that conveys information about volatile chemical odorants related to food (Endo et al., 2007; Martin et al., 2013; Mosca and Luo, 2014), throughout pupal (48–92 h APF) development (Fig. 7*B–F'*) and into adulthood from 0 to 24 d old (Fig. 7*G–O'*). We found that pupal Brp-Short puncta increased 1.5-fold from 48 to 72 h APF and then did not significantly change (Fig. 7*P*; Extended Data Table 7-1) throughout the rest of pupation. Pupal neurite volume also exhibited a nearly

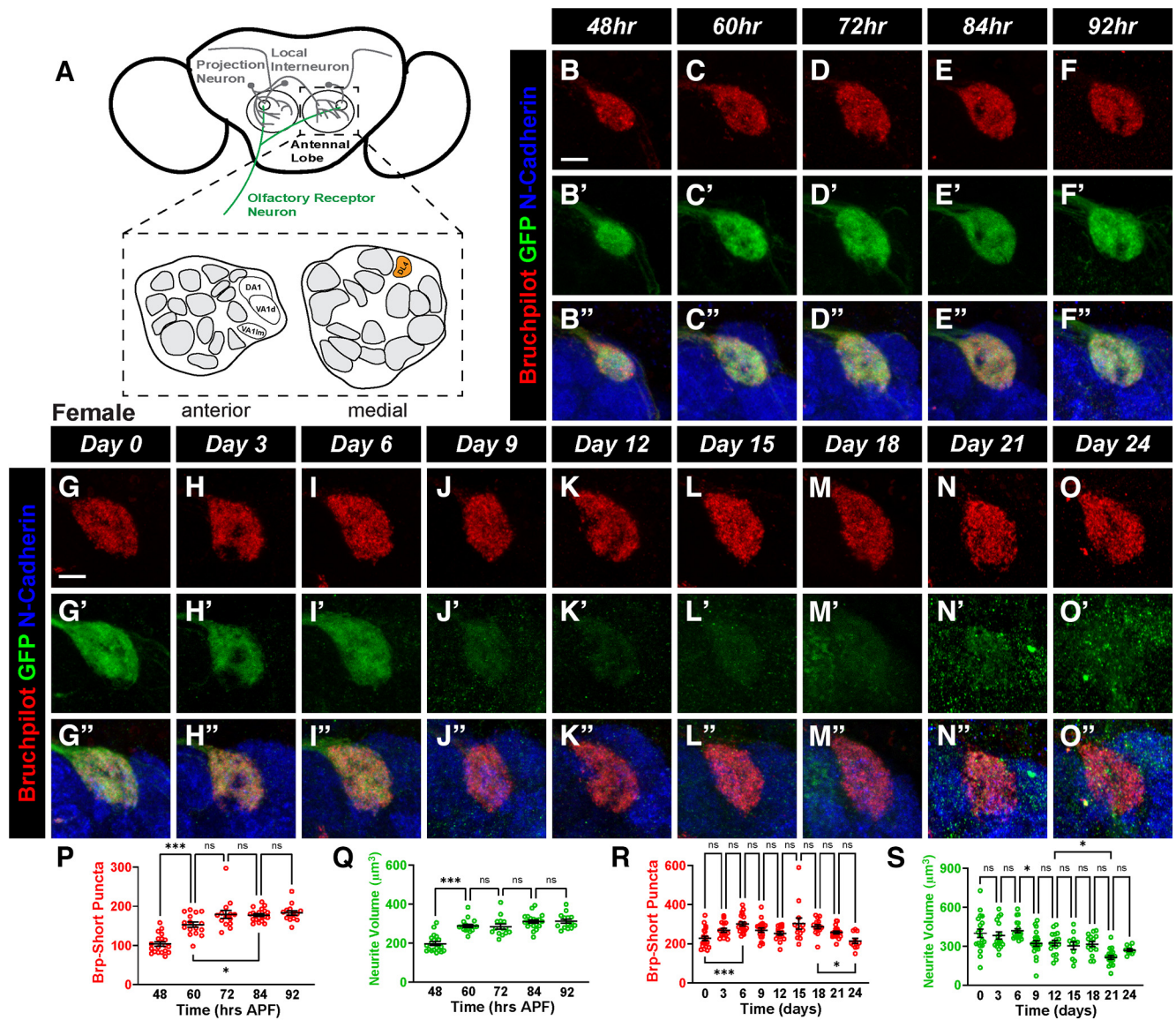


Figure 8. A developmental time course of synapse number and neurite volume in female DL4 ORNs. **A**, Schematic of the *Drosophila* antennal lobes showing ORNs (green) of the DL4 glomerulus (orange). **B–F''**, Representative confocal image stacks of female pupal DL4 ORNs expressing Brp-Short-mStraw and membrane-tagged GFP and stained with antibodies against mStraw (red), GFP (green), and N-cadherin (blue) at 48 h (**B**), 60 h (**C**), 72 h (**D**), 84 h (**E**), and 92 h (**F**) APF. **G–O''**, Representative confocal image stacks of female adult DL4 ORNs expressing Brp-Short-mStraw and membrane-tagged GFP and stained with antibodies as in **B–F''** at 0 d (**G**), 3 d (**H**), 6 d (**I**), 9 d (**J**), 12 d (**K**), 15 d (**L**), 18 d (**M**), 21 d (**N**), and 24 d (**O**) of age. **P, Q**, Quantification of Brp-Short-mStraw puncta (**P**) and membrane GFP volume (**Q**) for pupal female DL4 ORNs. Both synaptic puncta and neurite volume increase from 48 to 60 h APF. They then trend upward for the remainder of pupal development. **R, S**, Quantification of synaptic puncta (**R**) and neurite volume (**S**) for adult female DL4 ORNs. Synapses trend upward from 0 to 6 d old and then remain largely stable. Neurite volume remains steady until 12 d of age and then begins to decline. For each time point, $n \geq 10$ glomeruli from 5 brains. * $p < 0.1$, *** $p < 0.001$, ns = not significant. Scale bar = 5 μm . Raw data are provided in Extended Data Table 8-1.

1.5-fold change from 48 to 72 h APF before reaching a steady-state neurite volume that was maintained until adulthood (Fig. 7Q; Extended Data Table 7-1), suggesting much of the development of pupal DL4 ORNs occurs well in advance of eclosion. Adult male Brp-Short puncta in DL4 ORNs significantly increased by 1.25-fold from 0 to 12 d after eclosion before achieving their mature synapse number and maintaining that number of puncta throughout the remainder of observed adulthood (Fig. 7R; Extended Data Table 7-1), further demonstrating that synapse formation continues into adulthood. Adult neurite volume did not significantly change from 0 to 6 d after eclosion, maintaining a similar level to that measure during pupal stages; intriguingly, however, neurite volume declined from 6 to 15 d by 39% and from 18 to 21 d by 60% (Fig. 7S; Extended Data Table 7-1).

We additionally generated a time course of development for female DL4 ORNs (Fig. 8A–O'') to examine any potential sexual dimorphism. Female DL4 ORNs showed a 1.5-fold increase in both Brp-Short puncta (Fig. 8P; Extended Data Table 8-1) and neurite volume (Fig. 8Q; Extended Data Table 8-1) from 48 to 60 h APF with no significant changes for the remainder of pupal development. Adult female DL4 Brp-Short puncta significantly increased between 0 and 6 d after eclosion by 33% before maintaining a steady-state. Brp-Short puncta then decreased by 25% from 18 to 24 d of age. (Fig. 8R; Extended Data Table 8-1). Female DL4 ORN adult neurite volume also did not significantly change from 0 to 6 d of age but significantly declined between 6 and 9 d (Fig. 8S; Extended Data Table 8-1). While neurite volume steadily decreased as the fly aged in both sexes, this is likely an

artificial effect of the *AM29-GAL4* driver weakening over time (Endo et al., 2007). We do not observe significant decrease of glomerular size in a general neuropil stain, suggesting volume remains largely constant. Overall, however, the absolute puncta numbers and neurite volumes at each stage were comparable between males and females, implying that synaptic development for food sensing ORNs is not sexually dimorphic and that both sexes use similar developmental programs for food-sensing ORNs. Thus, food-sensing ORNs use a different time course of synaptic development than pheromone-sensing glomeruli like DA1 and VA11m, one that emphasizes early development and lacks sexual dimorphism. Taken together, this indicates that ORNs of sexually dimorphic glomeruli follow similar rules for synaptic development which are distinct from the rules followed by nonsexually dimorphic ORNs and that within classes, each ORN subtype has subtle, individual variations in development.

Projection neurons continually develop synapses during pupation and early adulthood

Projection neurons (PNs) comprise the second order neurons of the olfactory system, relaying odorant information from ORNs that project onto PN dendrites in the antennal lobe to higher order brain structures such as the mushroom bodies and the lateral horn (Modi et al., 2020). ORN to PN communication is vital for making behavioral decisions, including foraging, oviposition, and courtship, based on the odor information available to the fly (Jefferis et al., 2001). PNs also arrive in the antennal lobes before ORNs and begin prepatterning the various glomeruli in preparation for ORN arrival (Jefferis et al., 2004). Prior studies, however, have only examined wiring and not synapse formation. Wiring and synaptogenesis are separable but equally essential events, and despite the importance of these neurons, we lack a detailed understanding of how they develop synapses over time. We addressed this by constructing a time course of synapse formation for male DA1 PNs (Fig. 9A) using genetic access via the *Mz19-GAL4* driver (Jefferis et al., 2004); *Mz19-GAL4* drives expression in DA1, VA1d, and DC3 PNs, but we restricted our analysis to DA1 PNs to enable a direct comparison to the ORNs (and LNs, see below) of the same glomerulus (Figs. 4 and 5). This allowed us to assess whether different classes of neurons belonging to the same microcircuit, such as those observed within an olfactory glomerulus, would share developmental programs or use distinct modes of synapse addition. As with ORNs, we quantified Brp-Short puncta number and neurite volume from 48 to 92 h APF and from 0 to 24 d after eclosion (Fig. 9B–O). Unlike ORNs, however, Brp-Short puncta were clearly visible in PNs at 48 h APF and steadily increased in number over 2.5-fold by 92 h APF (Fig. 9P; Extended Data Table 9-1). Pupal neurite volume also continually increased during pupation, doubling from 48 to 92 h APF (Fig. 9Q; Extended Data Table 9-1). These data show that PN synapses develop throughout the course of pupation. During adulthood, Brp-Short puncta continued to be added after eclosion with puncta number increasing 2-fold from 0 to 6 d of age, followed by no significant changes for the rest of adulthood (Fig. 9R; Extended Data Table 9-1). Neurite volume increased nearly 2-fold from 0 to 3 d after eclosion and then remained largely unchanged throughout the rest of adulthood (Fig. 9S; Extended Data Table 9-1). Therefore, DA1 PNs develop synapses throughout pupation and even early into adulthood before stabilizing at their mature quantity. Unlike ORNs, however, they lack a pruning phase and reach their mature state more quickly.

We additionally generated a time course of development for female DA1 PNs to examine any potential sexual dimorphisms in PN synaptic development (Fig. 10A–O). In female PNs, both the number of Brp-Short puncta (Fig. 10P; Extended Data Table 10-1) and neurite volume increased 2-fold from 48 to 92 h APF (Fig. 10Q; Extended Data Table 10-1), showing that males and females both develop synapses during the entirety of pupation. Adult female PNs exhibited a nearly 2-fold increase in Brp-Short puncta from 0 to 6 d of age, and then did not change for the remainder of adulthood (Fig. 10R; Extended Data Table 10-1). Female neurite volume increased 1.5-fold from 0 to 3 d after eclosion and then did not significantly change (Fig. 10S; Extended Data Table 10-1; similar to males). These data demonstrate that male and female PNs have nearly identical time courses of synaptic development. Furthermore, their exact time frames of synapse addition and stabilization are distinct from those of ORNs. Therefore, PNs that receive information predominantly from pheromone-sensing ORNs have a unique pattern of synapse formation, demonstrating that different neuronal classes within the same microcircuit have distinct patterns of synaptic development. This may underlie their specific function in the antennal lobe olfactory circuit (see Discussion).

Local interneurons rapidly undergo synapse formation late in pupation to reach maturity

In the antennal lobe, the most diverse class of cells are local interneurons (Ng et al., 2002; Tanaka et al., 2008, 2012; Chou et al., 2010). Compared with ORNs and PNs, less is known about their precise physiological functions. LNs have been implicated in a number of processing steps in olfactory information including gain control, regulating interglomerular communication, and refining olfactory signal (Tanaka et al., 2009; Chou et al., 2010; Yaksi and Wilson, 2010; Hong and Wilson, 2015). Within the antennal lobe, different types of LNs synapse onto both ORN and PN targets. The multiglomerular LNs comprise the most numerous class and innervate multiple glomeruli throughout the antennal lobe. This innervation occurs after PN and ORN projections have entered the antennal lobes (Chou et al., 2010). Again, however, as wiring and synaptogenesis are separable events, there is little known about how synapse addition and active zone development occurs in these essential cells. Given their prominence among the olfactory LNs, we wanted to understand how their synapses developed. Therefore, we established a time course of synapse addition and neurite growth during development for a subset of multiglomerular LNs accessed genetically by *NP3056-GAL4* (Chou et al., 2010) for males (Fig. 11A) as well as females (Fig. 12A). To enable a direct comparison with Or67d-expressing ORNs and *Mz19*-accessed PNs, we focused our examination specifically to the projections of those multiglomerular LNs within the DA1 glomerulus (Fig. 11B–O). As *NP3056-GAL4* expresses in a heterogeneous population of LNs (Chou et al., 2010; Liou et al., 2018; Suzuki et al., 2020), these data represent the sum of all multiglomerular LN synapses in the DA1 glomerulus. This allowed us to compare synapse formation between each neuron class for the same precise region of the antennal lobe, eliminating cellular geography as a potential variable influencing synaptic development.

From 48 to 60 h APF, we observed very few LN synapses in DA1 and neurite elaboration within the glomerulus was minimal (Fig. 11B–C). Between 60 and 92 h APF, however, there was significant addition of active zones and neurite growth (Fig. 11D–F). In the final 30 h of pupation, active zone number increased

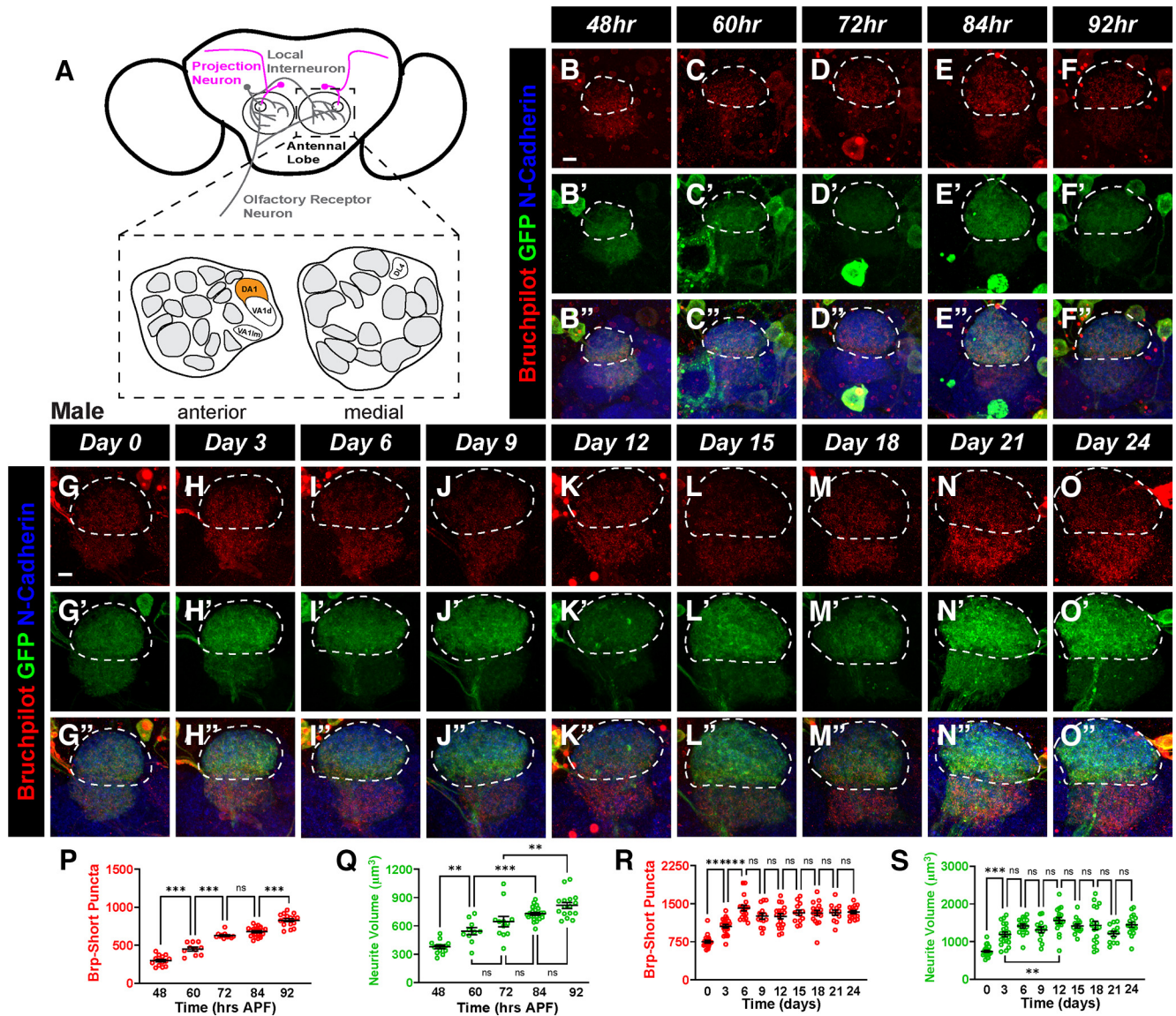


Figure 9. A developmental time course of synapse number and neurite volume in male DA1 projection neurons. **A**, Schematic of the antennal lobes showing PNs (magenta) of the DA1 glomerulus (orange). **B–F''**, Representative confocal image stacks of male pupal DA1 PNs (dashed white lines) expressing Brp-Short-mStraw and membrane-tagged GFP and stained with antibodies against mStraw (red), GFP (green), and N-cadherin (blue) at 48 h (**B**), 60 h (**C**), 72 h (**D**), 84 h (**E**), and 92 h (**F**) APF. **G–O''**, Representative confocal image stacks of male adult DA1 PNs (dashed white lines) expressing Brp-Short-mStraw and membrane-tagged GFP and stained with antibodies as in **B–F** at 0 d (**G**), 3 d (**H**), 6 d (**I**), 9 d (**J**), 12 d (**K**), 15 d (**L**), 18 d (**M**), 21 d (**N**), and 24 d (**O**) of age. **P, Q**, Quantification of Brp-Short-mStraw puncta (**P**) and membrane GFP volume (**Q**) for pupal male DA1 PNs. Brp-Short puncta and accompanying neurites are visible at 48 h APF and increase steadily during pupal development. **R, S**, Quantification of synaptic puncta (**R**) and neurite volume (**S**) for adult male DA1 PNs. Brp-Short puncta and neurite volume increase until 6 d after eclosion after which both stabilize for the remainder of adulthood. For each time point, $n \geq 10$ glomeruli from 5 brains. $**p < 0.01$, $***p < 0.001$, ns = not significant. Scale bar = 5 μm . Raw data are provided in Extended Data Table 9-1.

nearly 10-fold (Fig. 11P; Extended Data Table 11-1). LN neurite volume within DA1 also increased nearly 2.5-fold during the same time period (Fig. 11Q; Extended Data Table 11-1). We also determined the time course of synapse addition and neurite growth for multiglomerular LNs during the first 24 d of adulthood. At day 0, immediately after eclosion, we observed a higher number of active zones than at 92 h APF, indicating that even during the short time between 92 h APF and eclosion, there was a significant amount of synapse addition. The same was true of neurite outgrowth. Surprisingly, however, we found that both synapse number (Fig. 11R; Extended Data Table 11-1) and neurite outgrowth (Fig. 11S; Extended Data Table 11-1) remained constant from 0- to 24-d-old adult flies. Female DA1 LNs appeared nearly identical to male LNs (Fig. 12B–O''). From 60 to

92 h APF, female Brp-Short puncta increased 7-fold (Fig. 12P; Extended Data Table 12-1). In the same time frame, neurite volume increased 2-fold (Fig. 12Q; Extended Data Table 12-1). Female adult LNs differed from males in that Brp-Short puncta decreased 37% from 3 to 6 d of age and then re-increased 49% at 9 d of age (Fig. 12R; Extended Data Table 12-1). Neurite volume, however, did not change after eclosion (Fig. 12S; Extended Data Table 12-1). Overall, this suggests that LNs complete most synapse addition during pupal development. Males and females both showed the same general pattern of synapse formation, with the expected sex-specific dichotomy in synapse number and neurite volume (as observed previously in ORNs and PNs; Stockinger et al., 2005; Figs. 4, 5, 9, and 10). Female LNs, however, showed more variation throughout the adult time course

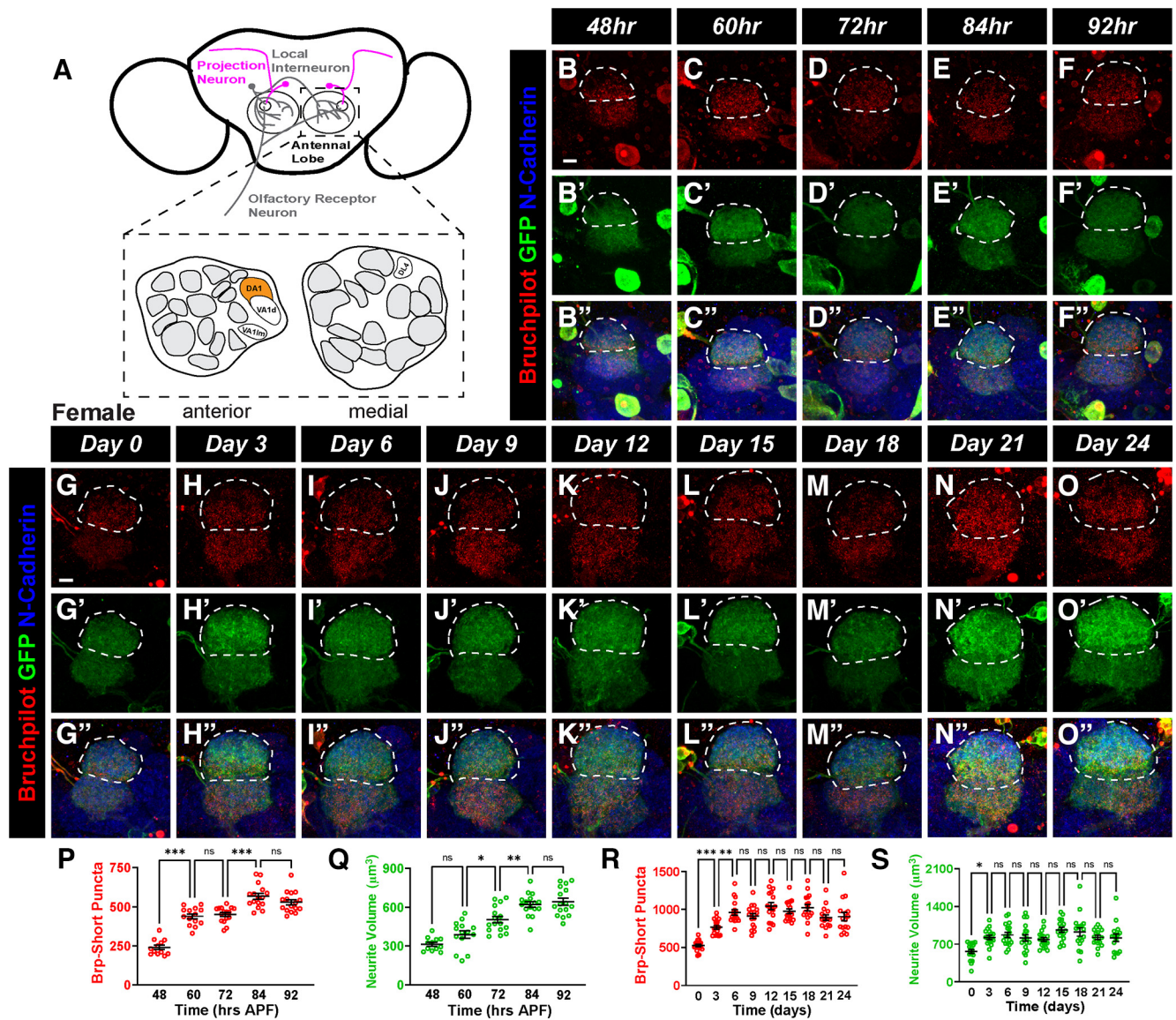


Figure 10. Synapse formation for female PNs of the DA1 glomerulus. *A*, Schematic of the antennal lobes showing PNs (magenta) of the DA1 glomerulus (orange). *B–F*’, Representative confocal image stacks of female pupal DA1 PNs (dashed white lines) expressing Brp-Short-mStraw and membrane-tagged GFP and stained with antibodies against mStraw (red), GFP (green), and N-cadherin (blue) at 48 h (*B*), 60 h (*C*), 72 h (*D*), 84 h (*E*), and 92 h (*F*) APF. *G–O*’, Representative confocal image stacks of female adult DA1 PNs (dashed white lines) expressing Brp-Short-mStraw and membrane-tagged GFP and stained with antibodies as in *B–F*’ at 0 d (*G*), 3 d (*H*), 6 d (*I*), 9 d (*J*), 12 d (*K*), 15 d (*L*), 18 d (*M*), 21 d (*N*), and 24 d (*O*) of age. *P, Q*, Quantification of Brp-Short-mStraw puncta (*P*) and membrane GFP volume (*Q*) for female pupal DA1 PNs. Synaptic puncta are added between 48 and 60 h APF as well as between 72 and 84 h APF. Neurite volume steadily increases until ~84–92 h APF. *R, S*, Quantification of synaptic puncta (*R*) and neurite volume (*S*) for female adult DA1 PNs. Synapses addition occurs from 0 to 6 d of age and then stabilizes. Neurite volume slightly increases from 0 to 3 d and the remains constant. For each time point, $n \geq 12$ glomeruli from 6 brains. * $p < 0.1$, ** $p < 0.01$, *** $p < 0.001$, ns = not significant. Scale bar = 5 μm . Raw data are provided in Extended Data Table 10-1.

than males, who retained their steady state of synapse number once achieved. This unique timeline of development for multi-glomerular LNs in the DA1 glomerulus highlights an additional developmental program that differs from the programs previously observed in ORNs and PNs.

Decreasing neuronal activity lowers synapse number in antennal lobe neurons

In a glomerular microcircuit, ORNs, PNs, and LNs have interconnected projections and fulfill distinct individual roles to support the larger goal of the antennal lobe in processing olfactory information. Our data suggest that each class of antennal lobe neurons, despite a shared goal and common microcircuit, utilizes different temporal programs to complete synaptic and neurite

development. As even closely related neurons of the same microcircuit use different developmental programs, this raised the possibility that each class of neurons may further use different molecular and cellular mechanisms to accomplish synaptic formation. One well-characterized modulator of synapse formation and plasticity is neuronal activity (Cang and Feldheim, 2013; Simi and Studer, 2018). Neurons with increased activity can out-compete other, less active neurons for synaptic partners as well as increase the number of synaptic connections made to other neurons (Miller, 1996). In *Drosophila*, there is a rich history of studying activity-dependent synaptic development at peripheral neuromuscular synapses (Keshishian et al., 1996); there, changes in activity influence synaptic development in terms of bouton number, ectopic projection, active zone organization,

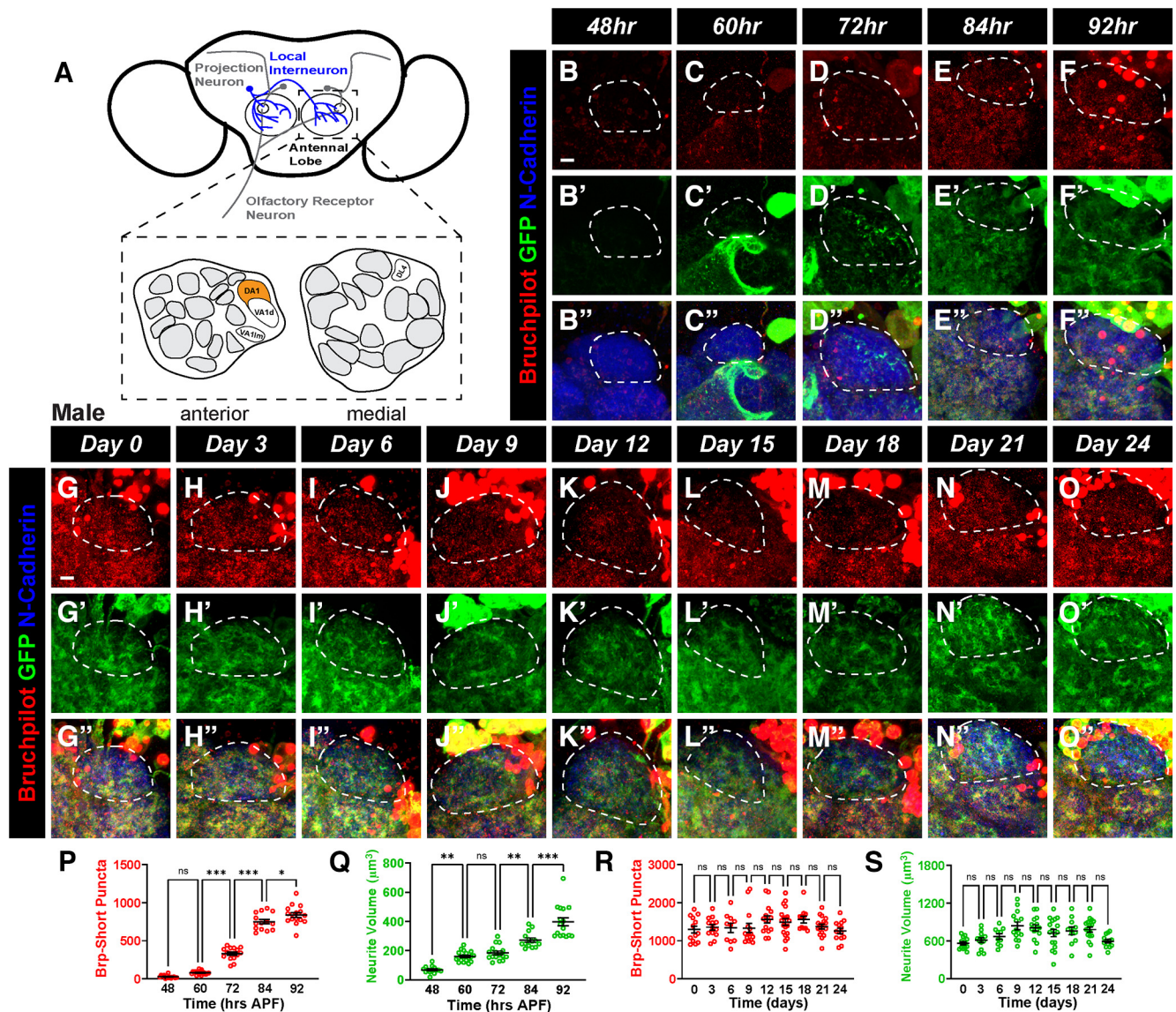


Figure 11. A developmental time course of male local interneuron synapse number and neurite volume in the DA1 glomerulus. **A**, Schematic of the antennal lobes showing LNs (blue) of the DA1 glomerulus (orange). **B–F''**, Representative confocal image stacks of male pupal DA1 LNs (dashed white lines) expressing Brp-Short-mStraw and membrane-tagged GFP and stained with antibodies against mStraw (red), GFP (green), and N-cadherin (blue) at 48 h (**B**), 60 h (**C**), 72 h (**D**), 84 h (**E**), and 92 h (**F**) APF. **G–O''**, Representative confocal image stacks of male adult DA1 LNs (dashed white lines) expressing Brp-Short-mStraw and membrane-tagged GFP and stained with antibodies as in **B–F''** at 0 d (**G**), 3 d (**H**), 6 d (**I**), 9 d (**J**), 12 d (**K**), 15 d (**L**), 18 d (**M**), 21 d (**N**), and 24 d (**O**) of age. **P, Q**, Quantification of Brp-Short-mStraw puncta (**P**) and membrane GFP volume (**Q**) for pupal male DA1 LNs. Synaptic puncta and neurites begin to significantly form between 60 and 72 h APF and rapidly increase for the remainder of pupal development. **R, S**, Quantification of synaptic puncta (**R**) and neurite volume (**S**) for adult male DA1 LNs. There is no significant difference in the number of synaptic puncta or neurite volume across all adult times examined. For each time point, $n \geq 10$ glomeruli from 5 brains. * $p < 0.05$, ** $p < 0.01$, *** $p < 0.001$, ns = not significant. Scale bar = $5 \mu\text{m}$. Raw data are provided in Extended Data Table 11-1.

and physiological output (Jarecki and Keshishian, 1995; Schmid et al., 2008; Harris and Littleton, 2015; Akin and Zipursky, 2020; Hazan and Ziv, 2020). The role of activity-dependent synapse organization in the CNS is less well understood, raising questions as to whether all synapses follow similar activity-dependent requirements for development or, as our temporal data might suggest, there is also heterogeneity within molecular and cellular programs that different central neurons use to complete development.

We first sought to determine whether antennal lobe neuron synapse development in ORNs, PNs, or LNs could be regulated by activity-dependent mechanisms. To accomplish this, we either decreased or increased neuronal activity chronically throughout development in ORNs, PNs, or LNs and quantified Brp-Short puncta number and neurite volume in those neurons. Because

our developmental analyses showed that ORNs, PNs, and LNs all achieved stable synapse number by 10 d after eclosion (Figs. 2–12), we specifically quantified synapse organization in 10-d-old adult flies. This allowed us to observe how changes in neuronal activity during development influence mature synapse density and to compare our findings between each neuron class. To decrease neuronal activity, we expressed an active tetanus toxin (TeTxLc) in either ORNs, PNs, or LNs that innervate the DA1 glomerulus and compared Brp-Short puncta numbers to neurons that expressed an inactive variant of the toxin as a control (Sweeney et al., 1995). Tetanus toxin lowers neuronal activity by cleaving Synaptobrevin at the synapse, impairing synaptic vesicle fusion and blocking neurotransmission (Sweeney et al., 1995). For male and female ORNs, there was a 29% and 21% decrease, respectively, in Brp-Short puncta number in neurons where active

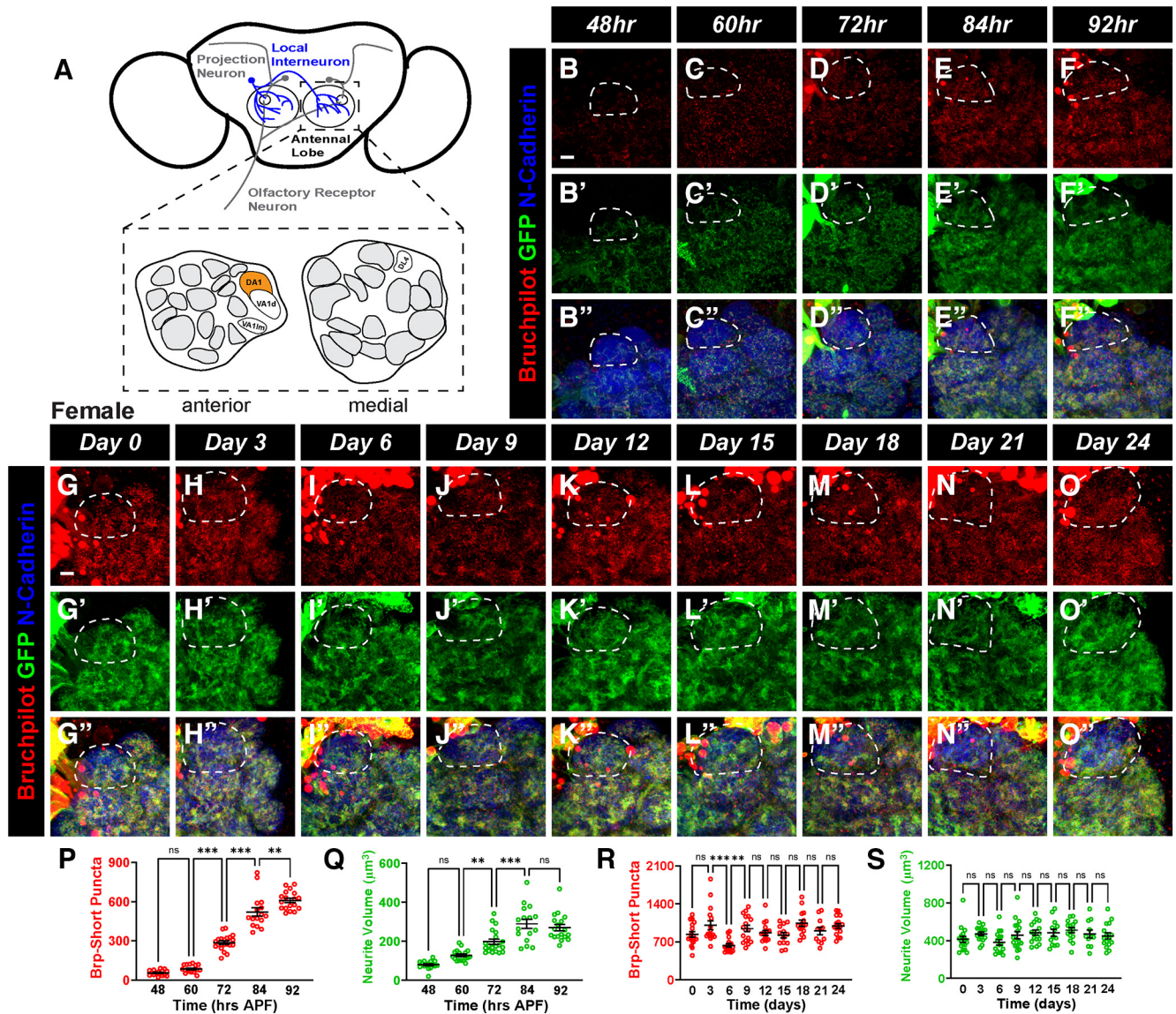


Figure 12. Synapse formation in the DA1 glomerulus for female LNs. **A**, Schematic of the antennal lobes showing LNs (blue) of the DA1 glomerulus (orange). **B–F'**, Representative confocal image stacks of female pupal DA1 LNs (dashed white lines) expressing Brp-Short-mStraw and membrane-tagged GFP and stained with antibodies against mStraw (red), GFP (green), and N-cadherin (blue) at 48 h (**B**), 60 h (**C**), 72 h (**D**), 84 h (**E**), and 92 h (**F**) APF. **G–O'**, Representative confocal image stacks of female adult DA1 LNs (dashed white lines) expressing Brp-Short-mStraw and membrane-tagged GFP and stained with antibodies as in **B–F'** at 0 d (**G**), 3 d (**H**), 6 d (**I**), 9 d (**J**), 12 d (**K**), 15 d (**L**), 18 d (**M**), 21 d (**N**), and 24 d (**O**) of age. **P, Q**, Quantification of Brp-Short-mStraw puncta (**P**) and membrane GFP volume (**Q**) for female pupal DA1 LNs. Addition of quantifiable synaptic puncta and neurite volume begins between 48 and 60 h APF and then occurs rapidly until 84–92 h APF. **R, S**, Quantification of synaptic puncta (**R**) and neurite volume (**S**) for female adult DA1 LNs. Synapses remain largely constant throughout adulthood, except for a decrease and subsequent increase from 3 to 9 d of age. Neurite volume is constant throughout adulthood. For each time point, $n \geq 11$ glomeruli from 6 brains. $^{**}p < 0.01$, $^{***}p < 0.001$, ns = not significant. Scale bar = 5 µm. Raw data are provided in Extended Data Table 12-1.

TeTxLc was expressed compared with the inactive control (Figs. 13A–B',G, 14A–B',G). However, neurite volume was unaffected by reduced activity (Figs. 13D–E',G, 14D–E',G). PNs also exhibited a significant decrease (by 60% for males and 36% for females) in Brp-Short puncta number following blocked synaptic transmission (Figs. 13H–I',N, 14H–I',N). Unlike ORNs, however, neurite volume was also significantly decreased in PNs expressing TeTxLc (Figs. 13K–L',N, 14K–L',N). Finally, we observed that TeTxLc expression in LNs caused a reduction in Brp-Short puncta (43% in males, 28% in females; Figs. 13O–P',U, 14O–P',U) but did not influence neurite volume (Figs. 13R–S',U, 14R–S',U). These data suggest that correct synapse addition requires a baseline level of neuronal activity, regardless of antennal lobe neuron class. However, PN neurite outgrowth appears to be activity dependent,

while ORN and LN neurite outgrowth seems to be activity independent.

We also sought to examine the consequences of reduced neuronal activity via a nonsynaptic method on synapse number. To do so, we expressed two copies of the transgenic Electrical Knock-out channel (2xEKO; White et al., 2001) in each olfactory neuron class. EKO is a modified *Drosophila* Shaker K⁺ channel that decreases neuronal excitability by activating at a low voltage (~–60 mV) for long periods of time, resulting in K⁺ influx and subsequent prevention of excitation (White et al., 2001). Similarly to TeTxLc, when 2xEKO was expressed in male and female ORNs, there was a 40% and 39% decrease in puncta number, respectively (Figs. 13C,C',G, 14C,C',G) without any change in neurite volume (Figs. 13F,F',G, 14F,F',G). In PNs, decreasing

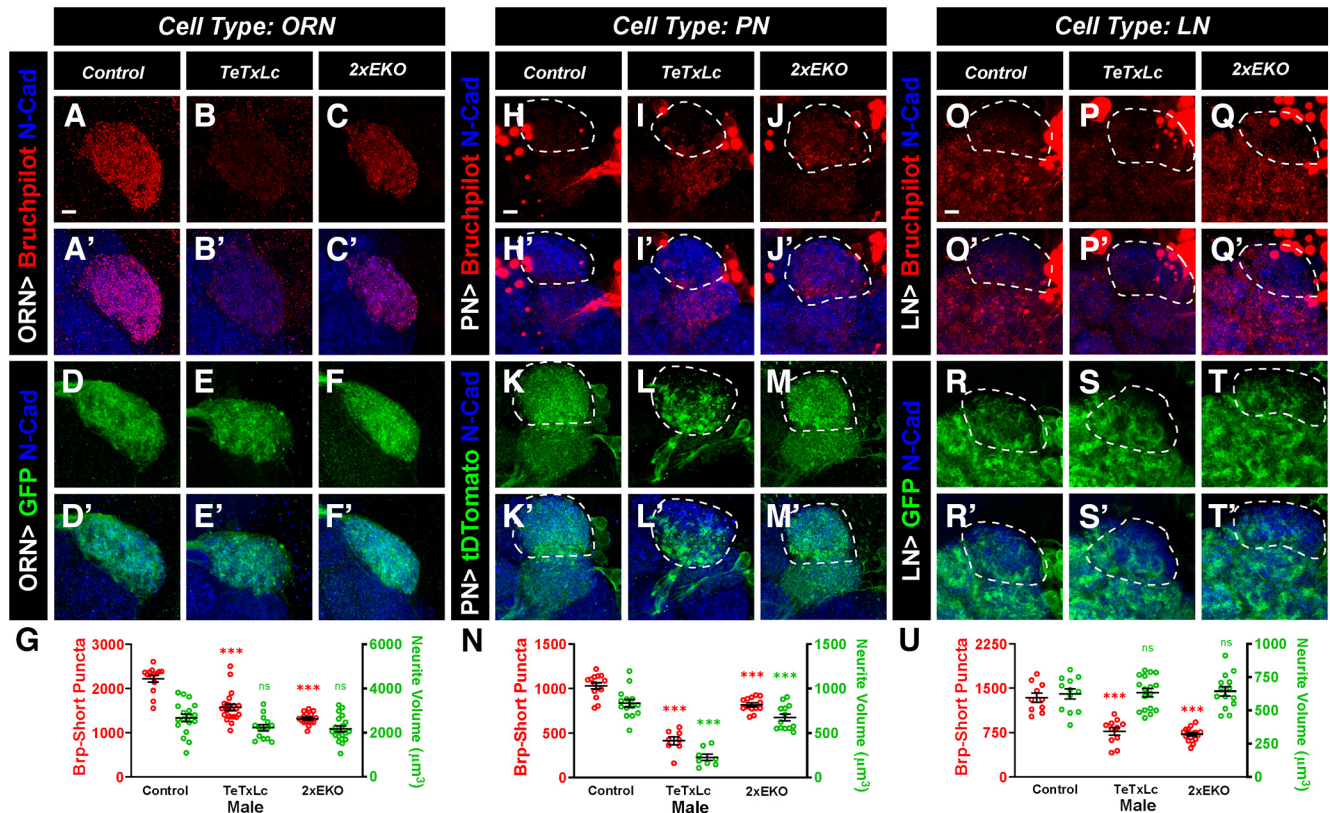


Figure 13. Normal neuronal activity is required for normal synaptic development in male ORNs, PNs, and LNs of the antennal lobe. *A–F*, Representative confocal image stacks of ORNs of the DA1 glomerulus expressing either Brp-Short-mStraw (*A–C*) or a membrane-tagged GFP (*D–F*) and either an inactive (*A, D*) variant of tetanus toxin light-chain (TeTxLc), an active (*B, E*) variant of TeTxLc, or two copies of EKO (*C, F*). Brains were stained with antibodies against mStraw (red) or GFP (green) and N-cadherin (blue). *G*, Quantification of Brp-Short puncta number and neurite volume between male DA1 ORNs expressing either active or inactive TeTxLc or 2xEKO. Expression of either active tetanus toxin or 2xEKO reduces the number of synaptic puncta without altering neurite volume. *H–M*, Representative image stacks of 10-d-old DA1 PNs (dashed white lines) expressing Brp-Short-GFP (*H–J*) or membrane-tagged tdtomato (*K–M*) and either inactive TeTxLc (*H, K*), active TeTxLc (*I, L*), or 2xEKO (*J, M*). Brains were stained with antibodies against tdtomato (green) or GFP (red) and N-cadherin (blue). *N*, Quantification of Brp-Short puncta number and neurite volume between male DA1 PNs expressing TeTxLc dead, TeTxLc active, or 2xEKO. Decreasing neuronal activity in PNs results in fewer synaptic puncta and reduced neurite volume. *O–T*, Representative image stacks of 10-d-old DA1 LNs (dashed white lines) expressing Brp-Short-mStraw (*O–Q*) or membrane-tagged GFP (*R–T*) as well as inactive TeTxLc (*O, R*), active TeTxLc (*P, S*), or 2xEKO (*Q, T*). Brains were stained with antibodies as in *A–F*. *U*, Quantification of Brp-Short puncta number and neurite volume between male DA1 LNs expressing TeTxLc dead, TeTxLc active, or 2xEKO. Decreasing neuronal activity in LNs decreased synaptic puncta but did not affect neurite volume. For each experimental group, $n \geq 8$ glomeruli from 4 brains. *** $p < 0.001$, ns = not significant. Scale bar = 5 μm .

neuronal excitability resulted in a reduction of Brp-Short puncta number (20% for males and 31% for females; Figs. 13*J, J', N, 14J, J', N*) as well as a significant decrease in neurite volume (Figs. 13*M, M', N, 14M, M', N*). Expression of 2xEKO in LNs also decreased the number of Brp-Short puncta similarly to blocking neurotransmission with TeTxLc (50% decrease in males and 25% decrease in females; Figs. 13*Q, Q', U, 14Q, Q', U*). However, decreasing excitability in female LNs reduced neurite volume by 25%, but did not affect male neurite volume (Figs. 13*T, T', U, 14T, T', U*). These results further indicate that synapse addition is dependent on a baseline level of neuron activity across all antennal lobe neuron classes, but that neurite growth is activity dependent in PNs and largely activity independent in ORN and LN classes. This suggests that different activity-related mechanisms exist to control specific aspects of synapse organization in different classes of cells.

Increasing neuronal activity increases ORN but not PN or LN synapse formation

Neuronal activity regulates synapse formation and the strength of connections within neural circuits (Cang and Feldheim, 2013; Vonhoff and Keshishian, 2017; Simi and Studer, 2018; Pan and Monje, 2020). We established that reduced neural activity results

in fewer synapses in all classes of neurons observed and sought next to determine whether the reciprocal relationship was true for antennal lobe neurons: does increased electrical activity result in additional synapses? To increase neuronal activity in DA1 ORNs, PNs, and LNs, we expressed the bacterial sodium channel NaChBac, which increases electrical activity by enhancing the inward Na^+ current into the cells, resulting in additional action potentials and neuronal firing (Ren et al., 2001; Nitabach et al., 2006). We observed that NaChBac expression in male or female DA1 ORNs (Figs. 15*A–D', 16A–D'*) led to a 49% or 38% increase, respectively, in Brp-Short puncta (Figs. 15*E, 16E*) but did not significantly alter neurite volume (Figs. 15*E, 16E*). This suggests a direct relationship between cell-autonomous neuronal activity and ORN synapse formation. Intriguingly, we found that this relationship did not exist in PNs: NaChBac expression in DA1 PNs had no effect on either Brp-Short puncta number (Figs. 15*F–G', 16F–G', J*) or neurite volume (Figs. 15*H–I', 16H–I', J*) in males or females. This suggests that PN synapse formation is resistant to increases in electrical activity, but sensitive to reduced neuronal firing, indicating partial activity dependence. Finally, NaChBac expression in LNs exhibited sexually dimorphic changes in synapse number. Increased LN activity in males had no effect on Brp-Short puncta number (Fig. 15*K–L', O*) or

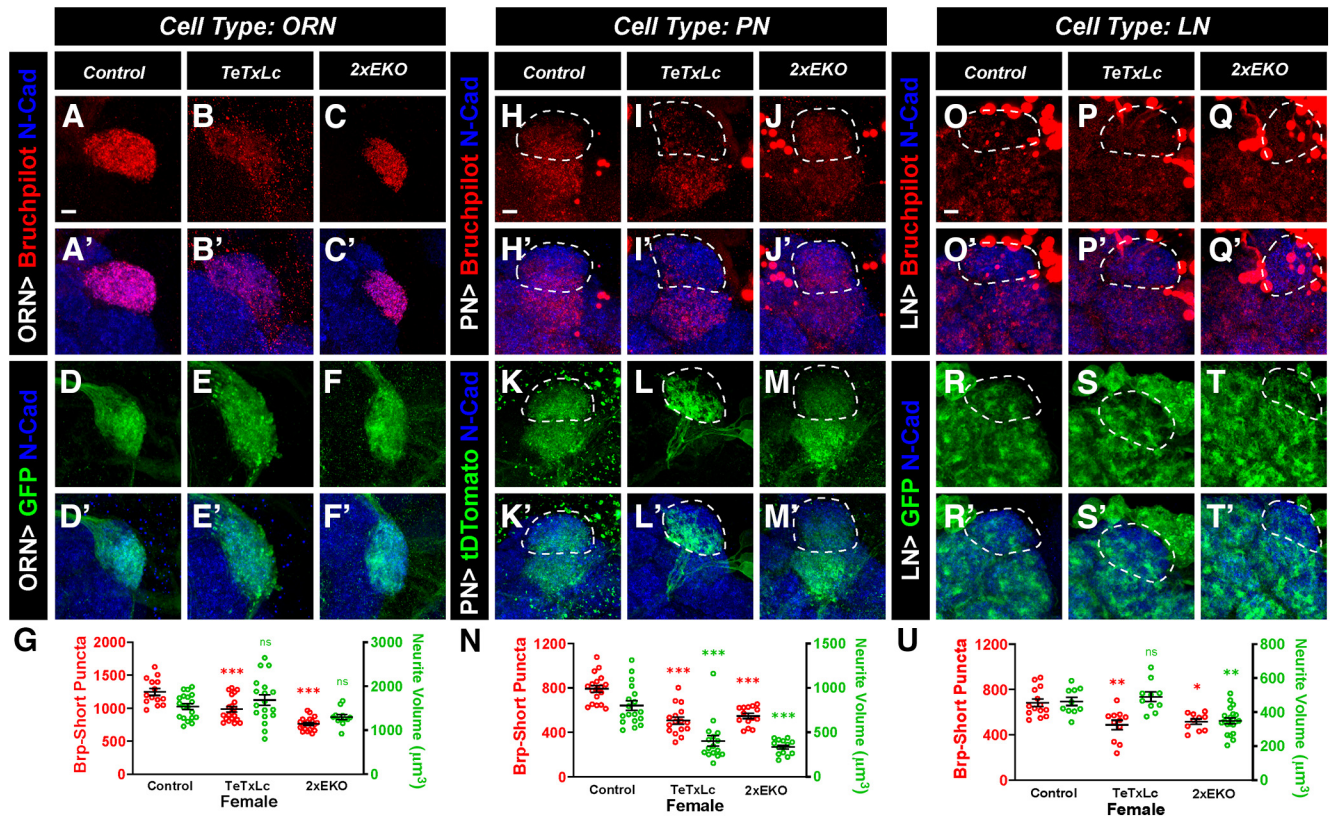


Figure 14. Decreasing neuronal activity in female antennal lobe neurons of the DA1 glomerulus. **A–F**, Representative confocal image stacks of ORNs of the DA1 glomerulus expressing either Brp-Short-mStraw (**A–C**) or a membrane-tagged GFP (**D–F**) and either an inactive variant of TeTxLc (**A, D**), an active variant of TeTxLc (**B, E**), or 2xEKO (**C, F**). Brains were stained with antibodies against mStraw (red) or GFP (green) and N-cadherin (blue). **G**, Quantification of Brp-Short puncta number and neurite volume between female DA1 ORNs expressing either active or inactive TeTxLc or 2xEKO. Expression of active tetanus toxin or 2xEKO reduces the number of synaptic puncta without altering neurite volume. **H–M**, Representative image stacks of 10-d-old DA1 PNs (dashed white lines) expressing Brp-Short-GFP (**H–J**) or membrane-tagged tdtomato (**K–M**) and either inactive TeTxLc (**H, K**), active TeTxLc (**I, L**), or 2xEKO (**J, M**). Brains were stained with antibodies against tdtomato (green) or GFP (red) and N-cadherin (blue). **N**, Quantification of Brp-Short puncta number and neurite volume between female DA1 PNs expressing TeTxLc dead, TeTxLc active, or 2xEKO. Decreasing neuronal activity in PNs results in fewer synaptic puncta and reduced neurite volume. **O–T**, Representative image stacks of 10-d-old DA1 LNs (dashed white lines) expressing Brp-Short-mStraw (**O–Q**) or membrane-tagged GFP (**R–T**) as well as inactive TeTxLc (**O, R**), active TeTxLc (**P, S**), or 2xEKO (**Q, T**). Brains were stained with antibodies as in **A–F**. **U**, Quantification of Brp-Short puncta number and neurite volume between female DA1 LNs expressing inactive TeTxLc, TeTxLc active, or 2xEKO. Decreasing synaptic transmission in LNs decreased synaptic puncta but did not affect neurite volume. Decreasing excitability in LNs also decreased synaptic puncta as well as neurite volume. For each experimental group, $n \geq 10$ glomeruli from 5 brains. * $p < 0.1$, ** $p < 0.01$, *** $p < 0.001$, ns = not significant. Scale bar = $5 \mu\text{m}$.

neurite volume (Fig. 15M–O) but significantly reduced Brp-Short puncta (Fig. 16K–L',O) in females by 19% without altering neurite volume (Fig. 16M–O). This indicates a number of aspects about the relationship between LN synapse formation and neural activity: (1) that there is a sexual dimorphism between males and females in the activity dependence of synapse formation; (2) in females, there is likely to be an optimal electrical activity that promotes synapse formation whereby any alteration (increase or decrease) results in impaired synapse formation; and (3) in males, there is likely to be some level of independence from increased activity in regulating synapse formation but sensitivity to reduced activity in regulating synapse formation (similar to PNs but in contrast to ORNs). Collectively, these results demonstrate that each class of neuron is influenced differently by increased neuronal activity and that the rules that govern synapse development are not the same for each class of neuron.

Altering kinase activity affects synapse number differently in ORNs compared with PNs and LNs

Diverse signal transduction and molecular pathways are responsible for translating changes in neuronal activity to cellular modifications in neurons, including altered neurite volume, synapse number, and gene expression (Chiang et al., 2009; Heinz and

Bloodgood, 2020; Faust et al., 2021; Lee and Fields, 2021). Our data suggested that perturbing electrical activity had both shared and differential effects on synapse formation across distinct neuronal class (ORN vs PN vs LN): reduced electrical activity reduced synapse number in all classes, but increased electrical activity affected synapse number in some (ORN) but not all (PN and LN) neuronal classes. We next sought to identify a molecular determinant that could underlie at least some of the changes we observed in activity-related synapse number. Shaggy (*sgg*), the *Drosophila* homolog of the mammalian kinase GSK-3 β , functions with neuronal activity to mediate neuronal stability in the CNS (Chiang et al., 2009) and at the NMJ to regulate bouton formation and microtubule organization (Franco et al., 2004; Ataman et al., 2008; Miech et al., 2008). However, it is unclear whether kinase activity influences synapse formation in addition to neuronal stability. In ORNs, there is an inverse relationship between neuronal activity and *sgg* kinase levels, whereby increased neuronal activity leads to decreased kinase activity, promoting axon stability, while decreased neuronal activity leads to increased kinase levels and axon degeneration (Chiang et al., 2009). Our data indicates that ORN, PN, and LN synapse number are all reduced when neuronal activity is decreased (Figs. 13 and 14). Thus, we hypothesized that if Shaggy was the

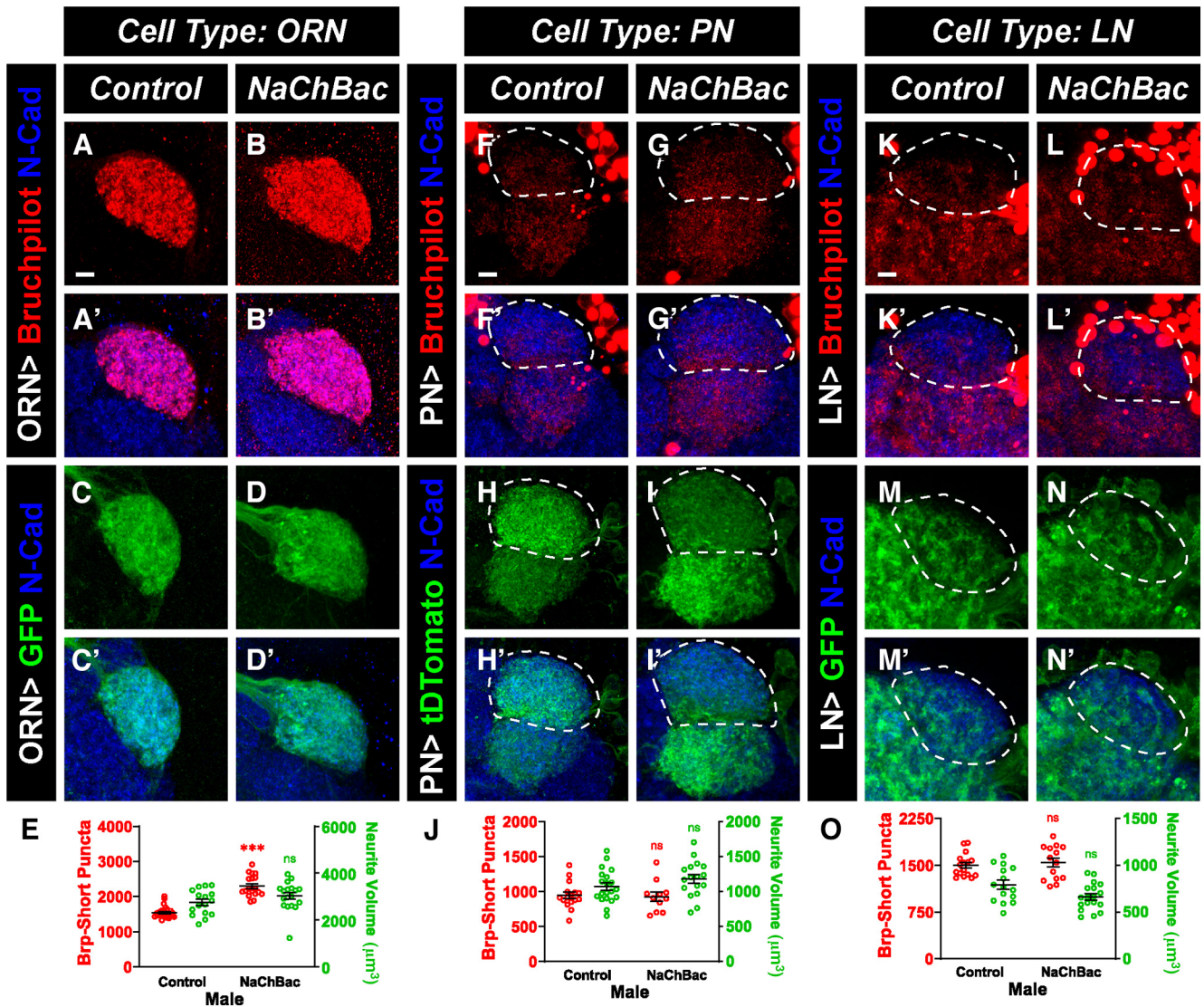


Figure 15. Increased neuronal activity in male ORNs, but not PNs or LNs, results in an increase in synapse number. **A–D'**, Representative confocal image stacks of 10-d-old DA1 ORNs expressing either Brp-Short-mStraw (**A, B**) or membrane-tagged GFP (**C, D**) in control flies (**A, C**) or in flies expressing the NaChBac (**B, D**) construct to increase neuronal activity. Brains were stained with antibodies against mStraw (red) or GFP (green) and N-cadherin (blue). **E**, Quantification of Brp-Short puncta and neurite volume in control and NaChBac expressing male DA1 ORNs. Increasing neuronal activity increased the number of synaptic puncta without affecting neurite volume. **F–I'**, Representative image stacks of 10-d-old DA1 PNs (dashed white lines) expressing Brp-Short-GFP (**F, G**) or membrane-tagged tdtomato (**H, I**) in control (**F, H**) or NaChBac expressing (**G, I**) flies. Brains were stained with antibodies against tdtomato (green) or GFP (red) as well as N-cadherin (blue). **J**, Quantification of Brp-Short puncta and neurite volume for control male DA1 PNs or those expressing NaChBac. Increasing neuronal activity in PNs did not affect synaptic puncta number or neurite volume. **K–N'**, Representative image stacks of 10-d-old DA1 LNs (dashed white lines) expressing Brp-Short-mStraw (**K, L**) or membrane-tagged GFP (**M, N**) in control (**K, M**) or NaChBac expressing (**L, N**) flies with antibody staining as in **A–D'**. **O**, Quantification of Brp-Short puncta and neurite volume for male DA1 LNs. Increasing excitability did not affect puncta number or neurite volume. For each experimental group, $n \geq 11$ glomeruli from 6 brains. *** $p < 0.001$, ns = not significant. Scale bar = 5 µm.

relevant downstream kinase to mediate these changes in synapse number (and given the inverse relationship between neuronal activity and kinase levels), overexpression of a constitutively active *sgg* (*sgg-CA*) would result in a similar reduction in synapse number. To test this, we expressed a constitutively active variant of *sgg* (*Sgg-CA*; Bourouis, 2002) in all three classes of cells to increase kinase activity along with Brp-Short or mCD8-GFP to quantify synaptic puncta number and neurite volume. Consistent with this hypothesis, *Sgg-CA* expression in ORNs or LNs that innervate the DA1 glomerulus both similarly resulted in a cell autonomous decrease in Brp-Short puncta number in male (Fig. 17A–B', E, F–G', J) and female (Fig. 18A–B', E, F–G', J) brains. In male and female ORNs, neurite volume was unaffected (Figs. 17C–E, 18C–E), while in LNs, there was a 28% decrease in

neurite volume in males while female LN neurite volume was unaffected (Figs. 17H–J, 18H–J). We were unable to assess the effects of *Sgg-CA* expression on Brp puncta number in PNs as expression via *Mz19-GAL4* was lethal. This is likely because of constitutive developmental expression causing lethality, as previously observed (Berdnik et al., 2006). This ORN and LN data, however, supports the hypothesis that electrical activity may signal through the GSK-3β homolog Shaggy to regulate olfactory synapse number across all observed classes of antennal lobe neurons. However, as male LN neurite volume is affected by *Sgg* activity but not neuronal activity (and vice versa for female LN neurite volume), there are also likely *Sgg*-dependent, activity-independent and *Sgg*-independent, activity-dependent phenomena that regulate neuronal growth.

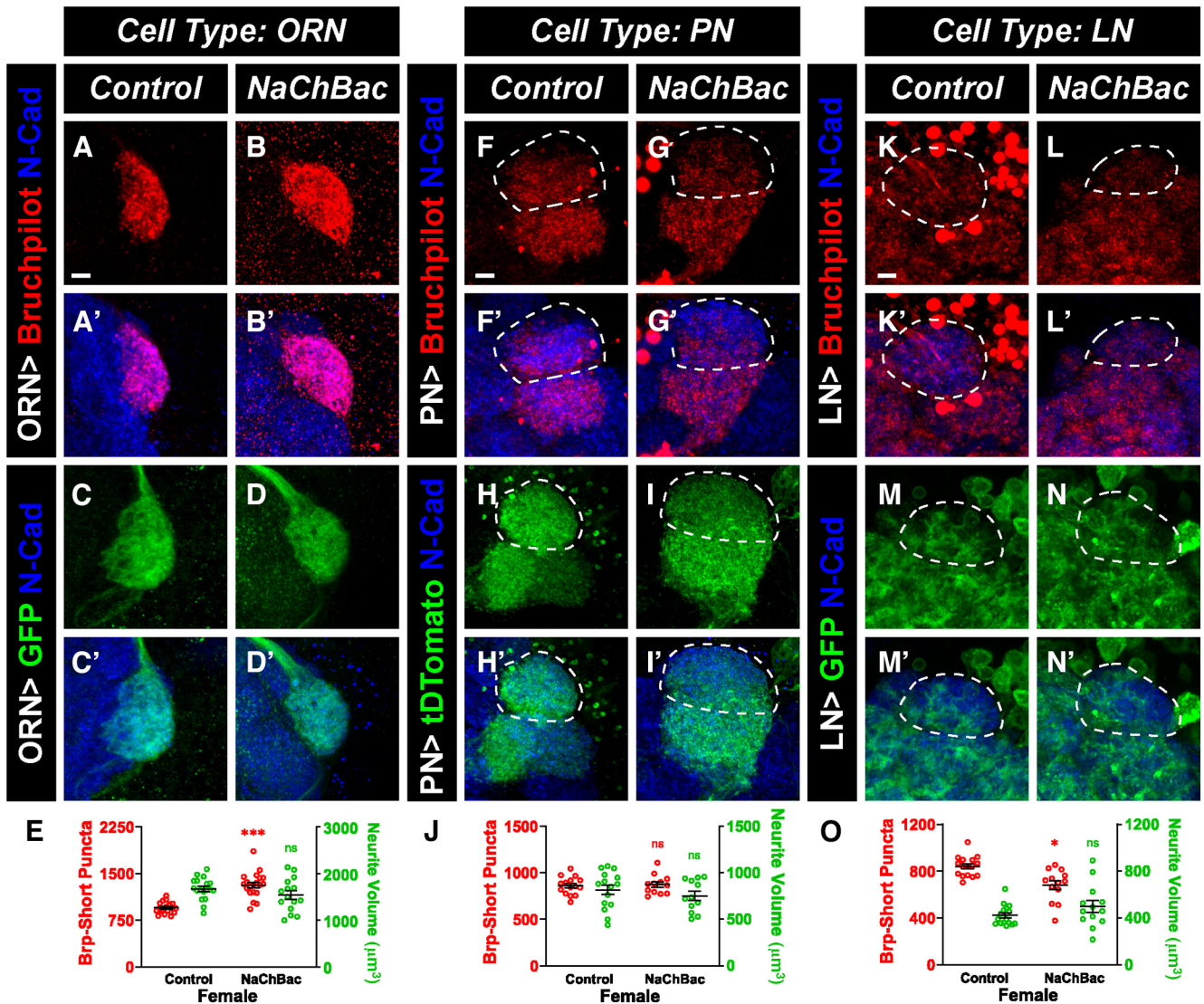


Figure 16. Increasing neuronal activity in female antennal lobe neurons of the DA1 glomerulus. *A–D'*, Representative confocal image stacks of 10-d-old DA1 ORNs expressing either Brp-Short-mStaw (*A, B*) or membrane-tagged GFP (*C, D*) in control flies (*A, C*) or in flies expressing a NaChBac (*B, D*) transgene to increase neuronal activity. Brains were stained with antibodies against mStaw (red) or GFP (green) and N-cadherin (blue). *E*, Quantification of Brp-Short puncta and neurite volume in control and NaChBac expressing female DA1 ORNs. Increasing neuronal activity increased the number of synaptic puncta without affecting neurite volume. *F–I'*, Representative image stacks of 10-d-old DA1 PNs (dashed white lines) expressing Brp-Short-GFP (*F, G*) or membrane-tagged tdtomato (*H, I*) in control (*F, H*) or NaChBac expressing (*G, I*) flies. Brains were stained with antibodies against tdtomato (green) or GFP (red) as well as N-cadherin (blue). *J*, Quantification of Brp-Short puncta and neurite volume for control female DA1 PNs or those expressing NaChBac. Increasing neuronal activity in PNs did not affect synaptic puncta number or neurite volume. *K–N'*, Representative image stacks of 10-d-old DA1 LNs (dashed white lines) expressing Brp-Short-mStaw (*K, L*) or membrane-tagged GFP (*M, N*) in control (*K, M*) or NaChBac expressing (*L, N*) flies with antibody staining as in *A–D'*. *O*, Quantification of Brp-Short puncta and neurite volume for female DA1 LNs. Increasing excitability slightly decreased puncta number without affecting neurite volume. For each experimental group, $n \geq 12$ glomeruli from 6 brains. * $p < 0.1$, *** $p < 0.001$, ns = not significant. Scale bar = 5 μm .

We similarly assessed the relationship between neuronal activity and kinase levels by expressing a dominant negative *sgg* transgene (*sgg-DN*) to decrease kinase levels (Franco et al., 2004). Because of the inverse relationship between the two activity levels, we hypothesized that decreasing Shaggy would phenocopy increasing neuronal activity. Intriguingly, however, decreasing kinase activity in ORNs decreased Brp-Short puncta in male (Fig. 19*A–B',E*) and female (Fig. 20*A–B',E*) brains by 27% and 30%, respectively. However, decreasing *sgg* levels in PNs and LNs did not affect Brp-Short puncta in males (Fig. 19*F–G',J,K–L',O*) and females (Fig. 20*F–G',J,K–L',O*), matching the effects of increased excitability in these neuron classes. Decreased kinase activity increased neurite volume 26% in male PNs but did not affect ORNs or LNs (Fig. 19*C–E,H–J,M–O*) nor any class of neuron in females (Fig. 20*C–E,H–J,M–O*). This suggests additional

heterogeneity in the molecular cascades controlling neuronal and synapse development as well as sexual dimorphism. Overall, our data shows that development is not a uniform process between neuronal classes, even in neurons belonging to the same microcircuit with the same general processing goal, and that each class of neuron forms synapses using its own unique temporal, activity-dependent, and molecular programs. Thus, considerable temporal and molecular heterogeneity exists in the development of central synaptic organization.

Discussion

Synapse formation and maintenance are essential processes that begin during nervous system development and continue over the course of an animal's lifetime. Understanding how synapse

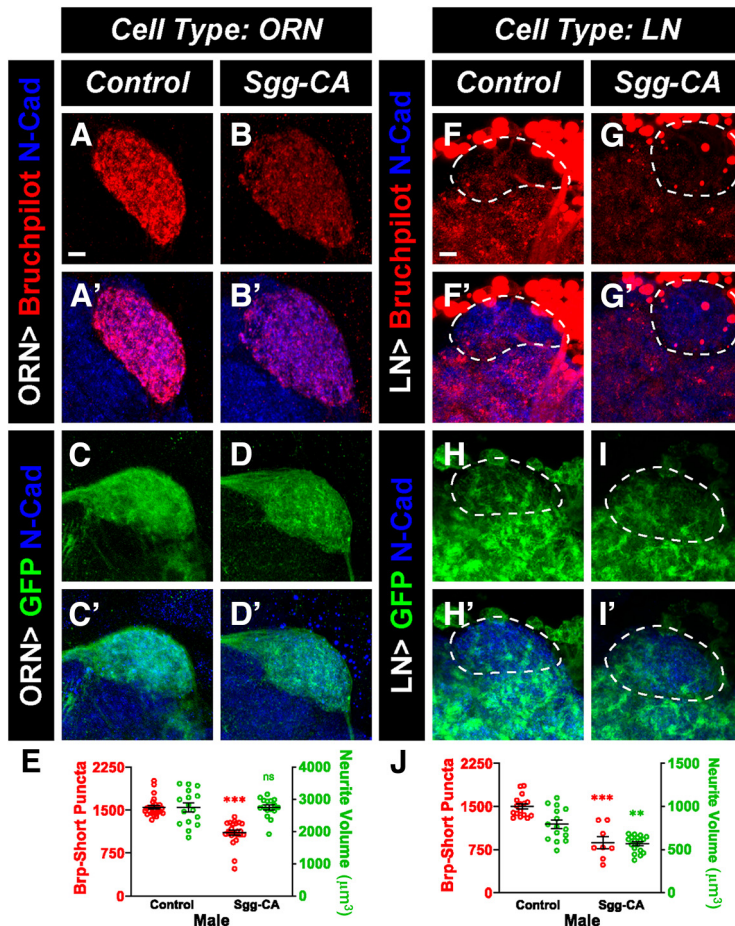


Figure 17. Increased kinase activity decreases male ORN and LN synapse number. *A–D'*, Representative confocal image stacks of 10-d-old ORNs of the DA1 glomerulus expressing Brp-Short-mStraw (*A, B*) or membrane-tagged GFP (*C, D*) in control flies (*A, C*) or in flies expressing a constitutively active (*B, D*) variant of Shaggy (*GSK3β*) to increase overall kinase activity. Brains were stained with antibodies against mStraw (red) or GFP (green) and N-cadherin (blue). *E*, Quantification of Brp-Short synaptic puncta and membrane GFP volume in control and Sgg-CA expressing male DA1 ORNs. Increasing kinase activity in ORNs caused a significant decrease in synaptic puncta but did not affect neurite volume. *F–I'*, Representative confocal image stacks of 10-d-old DA1 LNs (dashed white lines) expressing Brp-Short-mStraw (*F, G*) or membrane-tagged GFP (*H, I*) in control flies (*F, H*) or in flies expressing constitutively active (*G, I*) Shaggy and stained with antibodies as in *A–D'*. *J*, Quantification of Brp-Short puncta and neurite volume for control and Sgg-CA expressing male DA1 LNs. Increased activity decreased both puncta number and neurite volume in male DA1 LNs. For each experimental group, $n \geq 8$ glomeruli from 4 brains. * $p < 0.1$, ** $p < 0.01$, *** $p < 0.001$, ns = not significant. Scale bar = 5 μm.

organization changes during developmental and adult times is critical to understanding how different classes of cells employ temporal, molecular, and cellular programs to achieve proper development. As neuropsychiatric, neurodevelopmental, and even neurodegenerative disorders affect circuits at different times during the life cycle of an animal (Ilieva et al., 2009; Bennett, 2011; Grant, 2012; Bonansco and Fuenzalida, 2016; Mullins et al., 2016; Dabool et al., 2019), a clear picture of how different neurons, even neurons within the same circuit, develop is key to understanding how those disorders can influence circuit biology. Here, we have determined the first comprehensive timelines of active zone formation for three *Drosophila* olfactory neuron classes within the same microcircuit of the antennal lobe: olfactory receptor neurons, projection neurons, and local interneurons. Moreover, we also determined the developmental synaptic time courses for different subtypes of olfactory receptors that sense either food or pheromone odors. We find that each distinct class of olfactory neurons, despite having the same

overarching goal, to process olfactory information from the environment and transfer it to higher order brain centers to inform behavioral decisions, employs nonidentical temporal programs to accomplish synaptic development. We also demonstrate that development is still occurring during adult stages, up to as late as 6d after eclosion. Further, our data suggest that all three antennal lobe neuron classes share an activity-dependent component that influences synaptic development whereby reduced activity results in increased levels of *GSK-3β*, resulting in fewer synapses. Only ORNs increase synapse number in response to increased activity while synapse number in LNs and PNs remain unchanged following increased activity, suggesting divergence in activity-dependent mechanisms based on antennal lobe neuron class. Taken together, this indicates that synaptic development is not a uniform process for all neurons, with each neuron having its own time course of synapse formation depending on its class or subtype and that each class uses activity-dependent and activity-independent mechanisms differently to complete synaptic development. These results raise the importance of understanding the precise events in synaptic development for each class of neurons and the limitations of generalizing findings from one connection or neuronal class to another. By obtaining more detailed knowledge of how each neuron class develops in relation to others, including those within its own circuits, we gain a better understanding of each individual neuron class and can begin to determine the underlying genetic and molecular mechanisms that underlie these differences. This is essential to future developmental, molecular, and even degenerative studies to understand which and when events go awry during developmental disorders, why certain classes of neurons are more susceptible to damage or disease than others, and how different cells are organized to coordinate brain development.

Our findings suggest that developmental timing is not identical when comparing different classes or even subtypes of antennal lobe neurons. Each group of neurons has subtle, but clear, variations in how synapses are added or removed over time depending on its class and the type of olfactory information it relays. What is the evolutionary or ethological benefit of this? Why employ multiple temporal modes of development for the component neurons of a circuit that function together to promote a single sensory function? And why employ further developmental programs with different subtypes of the same neuronal class? ORNs that innervate the nonsexually dimorphic DL4 glomerulus are responsible for detecting food-based odorants (Couto et al., 2005; Endo et al., 2007). DL4 ORNs have a period of synapse formation from mid-pupation to 6d after eclosion followed by a plateau, thus maintaining a steady state number of synapses over the entire time observed (Figs. 7 and 8). In contrast to this, ORNs of the sexually dimorphic DA1 and VA1Im glomeruli, that are responsible for detecting pheromone-based odorants, instead show a period of rapid synaptic addition in early adulthood, followed by a decrease in synapses later in

adulthood (Figs. 2–5). This pattern of synapse formation is observed regardless of the specific active zone reporter quantified (Brp-Short or RIM-BP), indicating the generalizability of our findings (Fig. 6). In the case of the VA11m ORNs, this decrease appears to be caused by a pruning stage that is followed by maintenance of a steady state number of synapses. For DA1 ORNs, however, this occurs later in adulthood, perhaps as a period of senescence (Koch et al., 2021). It is tempting to speculate that these temporal patterns of synapse addition and removal may be related to the specific function of each class of ORNs. ORNs that detect food odorants and innervate nonsexually dimorphic glomeruli may retain the maximum synapse number throughout adulthood to ensure that the sensory abilities necessary to find food always exist. The need to locate and consume nutrients is a need that persists at all stages of the adult fly. ORNs that innervate sexually dimorphic glomeruli, like DA1 and VA11m, may instead lose connections as the animal ages because older flies exhibit reduced fecundity (Flatt, 2020) and the energetic cost of maintaining high synaptic numbers in a mate-seeking circuit may no longer be favored. Further, when PNs and LNs are considered with food-sensing or pheromone-sensing ORNs, why are there additional differences in developmental time courses? All ORN classes examined here and PNs increase synapses during the first 5–6 d of adult life before either plateauing at a steady state or pruning, then plateauing at a steady state (Figs. 2–10). LNs, however, develop their mature synaptic complement very quickly during pupation and are largely maintained from eclosion throughout adult life (Figs. 11 and 12). Female flies make the decision to lay their eggs in areas of resource richness (Aranha and Vasconcelos, 2018) to ensure that their progeny are born in areas that promote their survival. If olfactory acuity is connected to the number of synapses, and they spend their initial days of adult life in an area where there is ample food supply and other flies from other egg-laying females nearby, they may not have to rely on olfaction as much to find food and mates because of simple proximity to both during those initial days. However, when food resources become scarcer in the days following birth because of usage, and adult flies begin to travel further apart, the greater olfactory acuity afforded by an increase in synapse number is necessary to find new food sources and to locate mates over a larger geographical space. In such a situation, LNs may be immediately needed to control gain between ORNs and PNs and appropriate communication. ORNs and PNs, however, can attain their mature synapse number more slowly as peak acuity for transfer of the odorant information into the brain and conveyance of that information to higher brain centers is not needed until later in adult life. Further, as LNs regulate gain control of the AL circuit through connections with PNs and other LNs throughout adulthood, it is likely necessary for their synaptic connections to remain numerous throughout the fly's life

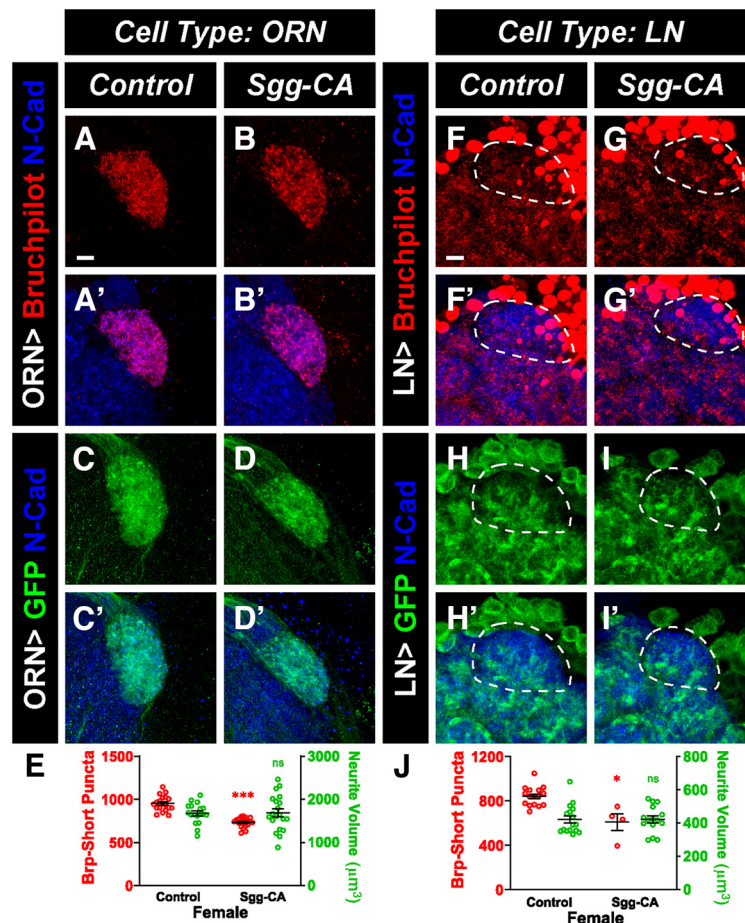


Figure 18. Increasing kinase activity in female olfactory neurons of the DA1 glomerulus only decreases synapse number. *A–D*, Representative confocal image stacks of 10-d-old female ORNs of the DA1 glomerulus expressing Brp-Short-mStraw (*A, B*) or membrane-tagged GFP (*C, D*) in control flies (*A, C*) or in flies expressing a constitutively active variant of Shaggy (*GSK3β*; *C, D*) to increase overall kinase activity. Brains were stained with antibodies against mStraw (red) or GFP (green) and N-cadherin (blue). *E*, Quantification of Brp-Short synaptic puncta and membrane GFP volume in female DA1 ORNs. Increasing kinase activity in ORNs caused a significant decrease in synaptic puncta but did not affect neurite volume. *F–I*, Representative image stacks of 10-d-old DA1 LNs (dashed white lines) expressing Brp-Short-GFP (*F, G*) or membrane-tagged tTomato (*H, I*) in control flies (*F, H*) or in flies expressing constitutively active Shaggy (*G, I*) and stained with antibodies as in *A–D*. *J*, Quantification of Brp-Short puncta and neurite volume for female DA1 LNs. Increased activity decreased puncta number without affecting neurite volume in female LNs. For each experimental group, $n \geq 4$ glomeruli from 2 brains. * $p < 0.1$, *** $p < 0.001$, ns = not significant. Scale bar = 5 μm .

without decline. Finally, the temporal differences may further be influenced by prior wiring events. There is a distinct order to ORN, PN, and LN wiring during pupation (Chou et al., 2010; Wilson, 2013; Sakuma et al., 2014; Liou et al., 2018), and although targeting events are largely complete by 48 h APF, neurite growth continues throughout pupal stages. With respect to synapse addition, PNs and ORNs had similar periods of synapse addition and plateau, but PN stages typically occurred slightly later than in ORNs. As LNs are the major targets of these connections (Schlegel et al., 2021), their later timing may be a result of the LNs being the last of the AL neurons to complete synaptic development. The PNs cannot begin forming presynapses until the LN projections have entered the glomerulus and have begun forming synapses of their own. Therefore, ORNs can begin forming synapses with the PNs immediately after they enter the glomerulus, but PN synapse formation may not be able to commence until LNs begin forming connections. In this consideration, the synaptic development of one class of neuron is partially

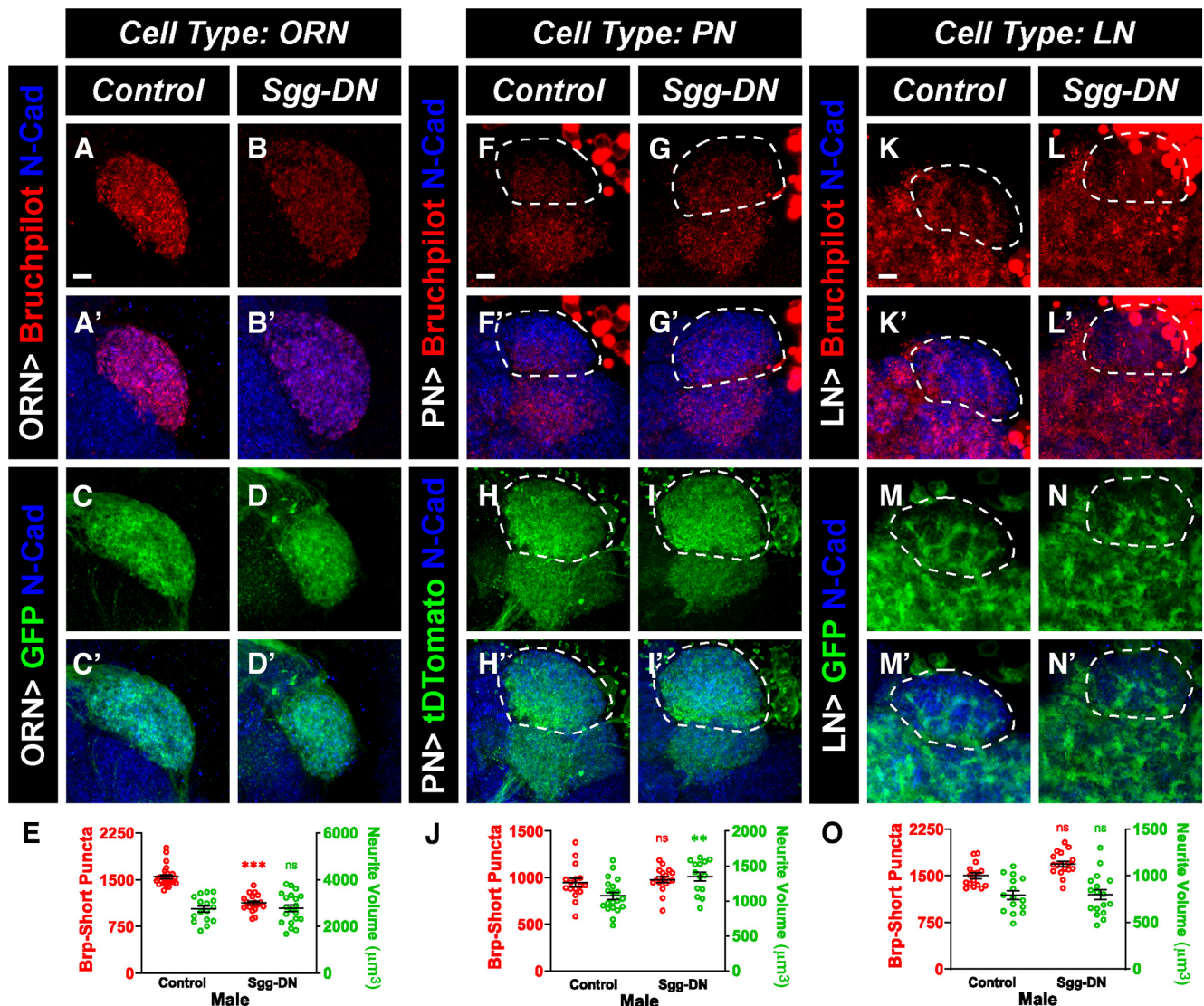


Figure 19. Decreasing kinase activity in male olfactory neurons decreases synapse number in ORNs, but not PNs or LNs. **A–D'**, Representative confocal image stacks of 10 d old male ORNs of the DA1 glomerulus expressing Brp-Short-mStraw (**A, B**) or membrane-tagged GFP (**C, D**) in control flies (**A, C**) or in flies expressing a dominant negative (**B, D**) variant of Shaggy (*GSK3 β*) to decrease overall kinase activity. Brains were stained with antibodies against mStraw (red) or GFP (green) and N-cadherin (blue). **E**, Quantification of Brp-Short synaptic puncta and membrane GFP volume in male DA1 ORNs of each group from **A–D'**. Decreasing kinase activity in ORNs caused a significant decrease in synaptic puncta but did not affect neurite volume. **F–I'**, Representative image stacks of 10-d-old male DA1 PNs (dashed white lines) expressing Brp-Short-GFP (**F, G**) or membrane-tagged tdTomato (**H, I**) in control flies (**F, H**) or in flies expressing dominant negative (**G, I**) Shaggy. Brains were stained with antibodies against tdTomato (green) or GFP (red) and N-cadherin (blue). **J**, Quantification of Brp-Short puncta and neurite volume in male DA1 PNs from **F–I'**. Decreasing kinase activity did not influence puncta number in PNs but did increase neurite volume. **K–N'**, Representative confocal image stacks of 10-d-old male DA1 LNs (dashed white lines) expressing Brp-Short-mStraw (**K, L**) or membrane-tagged GFP (**M, N**) in control flies (**K, M**) or in flies expressing dominant negative (**L, N**) Shaggy and stained with antibodies as in **A–D'**. **O**, Quantification of Brp-Short puncta and neurite volume for male DA1 LNs of the groups described in **K–N'**. Decreased kinase activity did not affect synaptic puncta or neurite volume in LNs. For each experimental group, $n \geq 14$ glomeruli from 7 brains. ** $p < 0.01$, *** $p < 0.001$, ns = not significant. Scale bar = 5 μm .

dependent on the development of the other neuron classes; this will be an interesting avenue for future study. Alternatively, the time courses of synapse formation may be dependent on different, more intrinsic developmental events. Development of synapses in a particular neuronal class may hinge on the time elapsed since the differentiation of that class from its progenitor cells or even from the initiation of neuronal activity rather than a global time point like pupal stage. Observing synaptic development from multiple time points and in multiple contexts may provide further insight into how different classes of neurons come together to form functioning circuits. Additional factors, including differential gene expression may also regulate the developmental events surrounding synapse addition and neurite growth. Our data suggest a

difference in the temporal aspects of synaptic development in sexually dimorphic pheromone-sensing glomeruli versus food-sensing glomeruli (Figs. 2–8). As the gene *fruitless* plays a significant role in regulating those pheromone-sensing glomeruli (Stockinger et al., 2005; Kurtovic et al., 2007; Datta et al., 2008; Tanaka et al., 2009), it is tempting to speculate that genes like *fru* may regulate differences in synapse formation as well. Overall, these detailed time courses demonstrate that even within the same circuit, different classes and subtypes of neurons have notable differences in their temporal programs of synaptic development. This highlights a previously unappreciated diversity in the development of central neurons and suggests that function, timing, and role may influence even similar neuron classes to

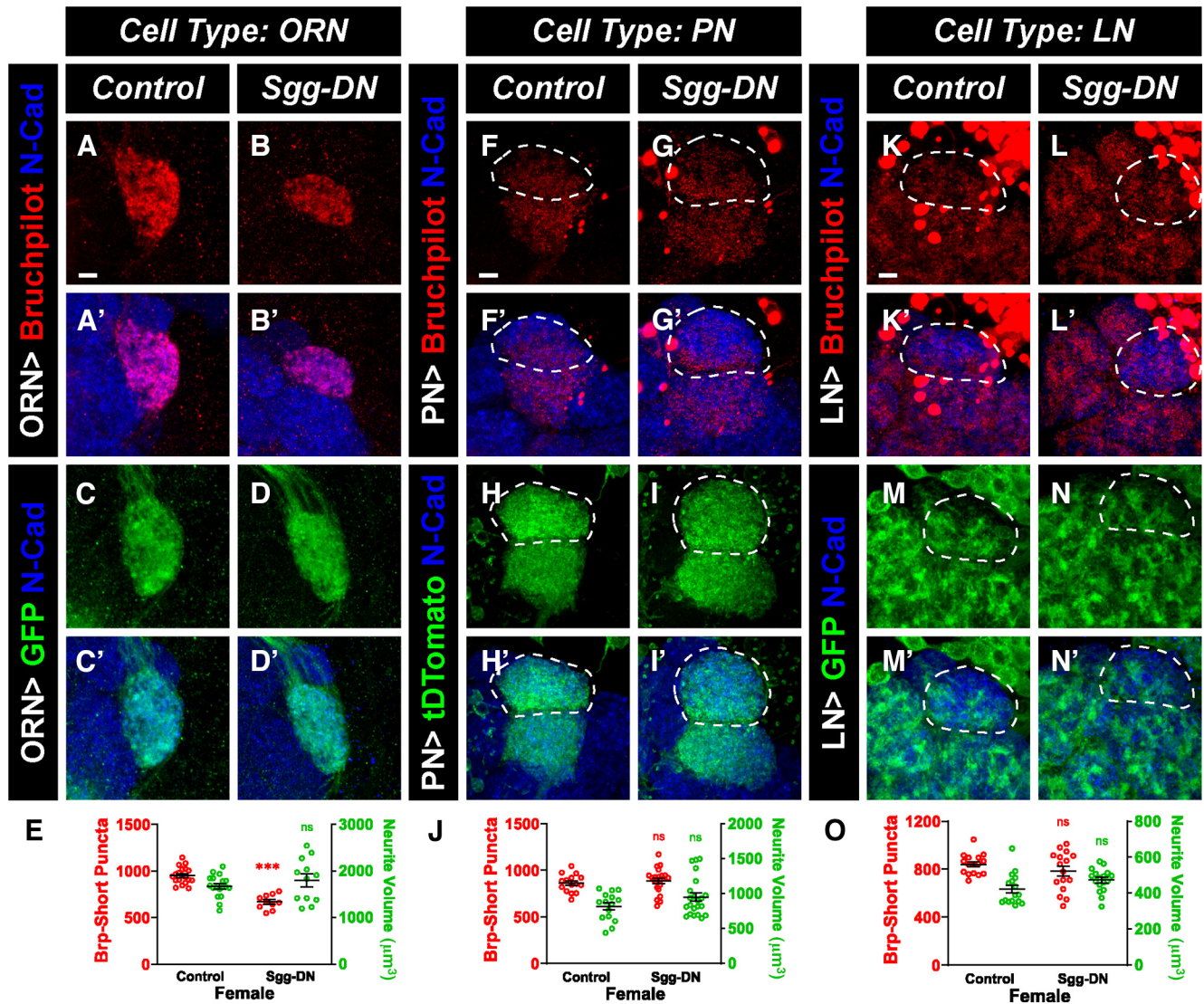


Figure 20. Decreasing kinase activity in female olfactory neurons of the DA1 glomerulus. *A–D'*, Representative confocal image stacks of 10-d-old female ORNs of the DA1 glomerulus expressing Brp-Short-mStraw (*A, B*) or membrane-tagged GFP (*C, D*) in control flies (*A, C*) or in flies expressing a dominant negative variant of Shaggy (*GSK3 β* ; *B, D*) to decrease overall kinase activity. Brains were stained with antibodies against mStraw (red) or GFP (green) and N-cadherin (blue). *E*, Quantification of Brp-Short synaptic puncta and membrane GFP volume in female DA1 ORNs. Decreasing kinase activity in ORNs caused a significant decrease in synaptic puncta but did not affect neurite volume. *F–I'*, Representative image stacks of 10-d-old DA1 PNs (dashed white lines) expressing Brp-Short-GFP (*F, G*) or membrane-tagged tdtomato (*H, I*) in control flies (*F, H*) or in flies expressing dominant negative (*G, I*) Shaggy. Brains were stained with antibodies against tdtomato (green) or GFP (red) and N-cadherin (blue). *J*, Quantification of Brp-Short puncta and neurite volume in female DA1 PNs. Decreasing kinase activity did not alter puncta number or neurite volume in PNs. *K–N'*, Representative confocal image stacks of 10-d-old DA1 LNs (dashed white lines) expressing Brp-Short-mStraw (*K, L*) or membrane-tagged GFP (*M, N*) in control flies (*K, M*) or in flies expressing dominant negative Shaggy (*L, N*) and stained with antibodies as in *A–D'*. *O*, Quantification of Brp-Short puncta and neurite volume for female DA1 LNs. Decreased kinase activity did not affect synaptic puncta or neurite volume in LNs. For each experimental group, $n \geq 10$ glomeruli from 5 brains. *** $p < 0.001$, ns = not significant. Scale bar = 5 μm .

use variant temporal programs during development to achieve mature circuit function.

Beyond temporal differences in the developmental programs used by different olfactory neuron classes, we also identified both similarities and differences in the activity-dependent and activity-independent molecular influences on synapse development. In ORNs, PNs, and LNs, we found that reduced neuronal activity results in fewer synapses, suggesting that a shared, baseline level of neuronal activity is generally necessary for complete synaptic development (Figs. 13 and 14). Previous work in the antennal lobe (Chiang et al., 2009) showed that decreased neuronal activity leads to increased activity of *shaggy*, the *Drosophila* GSK3 β homolog and leads to less axonal stability. Consistent with this, we find that overexpression of Sgg phenocopies the effects of

reduced neuronal activity in ORNs and LNs (Figs. 17 and 18; PN overexpression of Sgg is pupal lethal, precluding our analysis). In females, we did not observe any alterations to axonal stability with Sgg-CA overexpression, as neurite volume in ORNs and LNs remains unchanged. However, male LN neurite volume was affected by Sgg-CA expression. This suggests that this activity-dependent requirement for a baseline activity that functions through Sgg levels may be a common mechanism across olfactory neurons to control the development of active zone number. There is, however, a sexual dimorphism as to whether neurite volume is regulated by Sgg activity. Reduced electrical activity that results in increased kinase activity likely leads to more phosphorylation of downstream targets, resulting in removal of synapses. Whether this is a completely

cell autonomous phenomenon or is circuit-based, remains unclear. It will be important to test in the future whether different classes of neurons alter their synaptic development or growth when the activity of another neuronal class is impaired, possibly because of competition (Miller, 1996). Antennal lobe neurons showed different responses to increased electrical activity, however. Expression of NaChBac, a bacterial Na⁺ channel that increases neuronal firing, in ORNs resulted in more ORN synapses while either PN or LN expression of NaChBac had no effect on synapse number in those neurons (Figs. 15 and 16). This suggests that PNs and LNs are more resistant to activity increases compared with ORNs and that this may be an element of activity-independent regulation of synapse number. Alternatively, this may also indicate an upper limit on synapse number or to the extent by which neuronal activity influences synapse number. In ORNs, the downstream mechanism of how increased activity influences synapse number remains unclear. If a direct relationship existed between activity and GSK-3 β activity, we would expect that reducing kinase levels via expression of Sgg-DN would phenocopy the effects of NaChBac expression. Instead, Sgg-DN expression cell autonomously decreases synapse number in ORNs (Figs. 19 and 20). This highlights two major points: (1) there is an optimal level of Sgg activity in ORNs that influences synapse number and perturbations away from that optimal level impair synapse formation, and (2) there is an additional, yet undiscovered, mechanism that connects increased ORN activity with increased synapse number. In PNs and LNs, increased activity does not result in any changes to synapse number. Consistent with neuronal activity functioning through Sgg in these neurons, Sgg-DN expression in PNs or LNs also has no effect on synapse number. This represents a different mechanism for PNs and LNs than that which governs ORN synapse formation. This alternative mechanism for ORN synapse formation further highlights that the process of synaptic development is not uniform across all neuron types. Future work will therefore tease apart the activity-dependent and activity-independent mechanisms that influence synapse development in each class of neurons to understand how neuronal activity influences downstream cellular events, such as regulating kinase activity, to promote synapse formation and maintenance in distinct classes of neurons. Overall, our findings demonstrate the first synapse-level, quantitative analysis of presynaptic active zone development in each neuron class of a sensory circuit. These data increase our understanding of the rules that govern synaptic development and highlight critical caveats that should be considered for all future analyses of synaptic development and function. Developmental processes need to be uniquely understood for each class of neurons studied as our data indicates that there is no “one size fits all” rule for different classes of CNS neurons, even within the same circuit. Moreover, as synaptic development continues to occur during the adult stage, behavioral analyses need to be completed with appropriately age-matched controls and not spanning a range of ages, as this would compare neuronal function between neurons with different complements of presynaptic active zones and at different stages in their development. Taken together, these findings provide an essential bedrock from which future questions on the causes and consequences of incorrect development can be built and answered.

References

- Akin O, Zipursky SL (2020) Activity regulates brain development in the fly. *Curr Opin Genet Dev* 65:8–13.
- Aranha MM, Vasconcelos ML (2018) Deciphering *Drosophila* female innate behaviors. *Curr Opin Neurobiol* 52:139–148.
- Ataman B, Ashley J, Gorczyca M, Ramachandran P, Fouquet W, Sigrist SJ, Budnik V (2008) Rapid Activity-Dependent Modifications in Synaptic Structure and Function Require Bidirectional Wnt Signaling. *Neuron* 57:705–718.
- Baines RA, Bate M (1998) Electrophysiological development of central neurons in the *Drosophila* embryo. *J Neurosci* 18:4673–4683.
- Bennett MR (2011) Schizophrenia: susceptibility genes, dendritic-spine pathology and gray matter loss. *Prog Neurobiol* 95:275–300.
- Berdnik D, Chihara T, Couto A, Luo L (2006) Wiring stability of the adult *Drosophila* olfactory circuit after lesion. *J Neurosci* 26:3367–3376.
- Berger-Müller S, Sugie A, Takahashi F, Tavosanis G, Hakeda-Suzuki S, Suzuki T (2013) Assessing the role of cell-surface molecules in central synaptogenesis in the *Drosophila* visual system. *PLoS One* 8:e83732.
- Bonansco C, Fuenzalida M (2016) Plasticity of hippocampal excitatory-inhibitory balance: missing the synaptic control in the epileptic brain. *Neural Plast* 2016:8607038.
- Bourouis M (2002) Targeted increase in shaggy activity levels blocks wingless signaling. *Genesis* 34:99–102.
- Brand AH, Perrimon N (1993) Targeted gene expression as a means of altering cell fates and generating dominant phenotypes. *Development* 118:401–415.
- Cang J, Feldheim DA (2013) Developmental mechanisms of topographic map formation and alignment. *Annu Rev Neurosci* 36:51–77.
- Chiang A, Priya R, Ramaswami M, VijayRaghavan K, Rodrigues V (2009) Neuronal activity and Wnt signaling act through Gsk3- β to regulate axonal integrity in mature *Drosophila* olfactory sensory neurons. *Development* 136:1273–1282.
- Chin SG, Maguire SE, Huoviala P, Jefferis GSXE, Potter CJ (2018) Olfactory Neurons and Brain Centers Directing Oviposition Decisions in *Drosophila*. *Cell Rep* 24:1667–1678.
- Chou YHH, Spletter ML, Yaksi E, Leong JCSS, Wilson RI, Luo L (2010) Diversity and wiring variability of olfactory local interneurons in the *Drosophila* antennal lobe. *Nat Neurosci* 13:439–449.
- Christiansen F, Zube C, Andlauer TFM, Wichmann C, Fouquet W, Oswald D, Mertel S, Leiss F, Tavosanis G, Luna AJF, Fiala A, Sigrist SJ (2011) Presynapses in Kenyon cell dendrites in the mushroom body calyx of *Drosophila*. *J Neurosci* 31:9696–9707.
- Coates KE, Majot AT, Zhang X, Michael CT, Spitzer SL, Gaudry Q, Dacks AM (2017) Identified serotonergic modulatory neurons have heterogeneous synaptic connectivity within the olfactory system of *Drosophila*. *J Neurosci* 37:7318–7331.
- Coates KE, Calle-Schuler SA, Helmick LM, Knotts VL, Martik BN, Salman F, Warner LT, Valla SV, Bock DD, Dacks AM (2020) The wiring logic of an identified serotonergic neuron that spans sensory networks. *J Neurosci* 40:6309–6327.
- Collins CA, DiAntonio A (2007) Synaptic development: insights from *Drosophila*. *Curr Opin Neurobiol* 17:35–42.
- Couto A, Alenius M, Dickson BJ (2005) Molecular, anatomical, and functional organization of the *Drosophila* olfactory system. *Curr Biol* 15:1535–1547.
- Dabool L, Juravlev L, Hakim-Mishnaevski K, Kurant E (2019) Modeling Parkinson's disease in adult *Drosophila*. *J Neurosci Methods* 311:89–94.
- Dalva MB, McClelland AC, Kayser MS (2007) Cell adhesion molecules: signalling functions at the synapse. *Nat Rev Neurosci* 8:206–220.
- Datta SR, Vasconcelos ML, Ruta V, Luo S, Wong A, Demir E, Flores J, Balonze K, Dickson BJ, Axel R (2008) The *Drosophila* pheromone cVA activates a sexually dimorphic neural circuit. *Nature* 452:473–477.
- DePew AT, Mosca TJ (2021) Conservation and innovation: versatile roles for LRP4 in nervous system development. *J Dev Biol* 9:9.
- DePew AT, Aimino MA, Mosca TJ (2019) The tenets of teneurin: conserved mechanisms regulate diverse developmental processes in the *Drosophila* nervous system. *Front Neurosci* 13:27.
- de Ramon Francàs G, Zuñiga NR, Stoeckli ET (2017) The spinal cord shows the way - how axons navigate intermediate targets. *Dev Biol* 432:43–52.
- Endo K, Aoki T, Yoda Y, Kimura KI, Hama C (2007) Notch signal organizes the *Drosophila* olfactory circuitry by diversifying the sensory neuronal lineages. *Nat Neurosci* 10:153–160.
- Farhy-Tselnicker I, Allen NJ (2018) Astrocytes, neurons, synapses: a tripartite view on cortical circuit development. *Neural Dev* 13:7.
- Faust TE, Gunner G, Schafer DP (2021) Mechanisms governing activity-dependent synaptic pruning in the developing mammalian CNS. *Nat Rev Neurosci* 22:657–673.

- Fishilevich E, Vosshall LB (2005) Genetic and functional subdivision of the *Drosophila* antennal lobe. *Curr Biol* 15:1548–1553.
- Flatt T (2020) Life-history evolution and the genetics of fitness components in *Drosophila melanogaster*. *Genetics* 214:3–48.
- Fouquet W, Oswald D, Wichmann C, Mertel S, Depner H, Dyba M, Hallermann S, Kittel RJ, Eimer S, Sigrist SJ (2009) Maturation of active zone assembly by *Drosophila* Bruchpilot. *J Cell Biol* 186:129–145.
- Franco B, Bogdanik L, Bobinnec Y, Debec A, Bockaert J, Parmentier M-L, Grau Y (2004) Shaggy, the homolog of glycogen synthase kinase 3, controls neuromuscular junction growth in *Drosophila*. *J Neurosci* 24:6573–6577.
- Goda Y, Davis GW (2003) Mechanisms of synapse assembly and disassembly. *Neuron* 40:243–264.
- Grabe V, Sachse S (2018) Fundamental principles of the olfactory code. *Biosystems* 164:94–101.
- Grabe V, Baschwitz A, Dweck HKM, Lavista-Llanos S, Hansson BS, Sachse S (2016) Elucidating the neuronal architecture of olfactory glomeruli in the *Drosophila* antennal lobe. *Cell Rep* 16:3401–3413.
- Grant SGN (2012) Synaptopathies: diseases of the synaptome. *Curr Opin Neurobiol* 22:522–529.
- Hallem EA, Carlson JR (2006) Coding of odors by a receptor repertoire. *Cell* 125:143–160.
- Harris KP, Littleton JT (2015) Transmission, development, and plasticity of synapses. *Genetics* 201:345–375.
- Hazan L, Ziv NE (2020) Activity dependent and independent determinants of synaptic size diversity. *J Neurosci* 40:2828–2848.
- Heinz DA, Bloodgood BL (2020) Mechanisms that communicate features of neuronal activity to the genome. *Curr Opin Neurobiol* 63:131–136.
- Hibino H, Pironkova R, Onwumere O, Vologodskaja M, Hudspeth AJ, Lesage F (2002) RIM binding proteins (RBPs) couple Rab3-interacting molecules (RIMs) to voltage-gated Ca(2+) channels. *Neuron* 34:411–423.
- Hildebrand JG, Shepherd GM (1997) Mechanisms of olfactory discrimination: converging evidence for common principles across phyla. *Annu Rev Neurosci* 20:595–631.
- Hong EJ, Wilson RI (2015) Simultaneous encoding of odors by channels with diverse sensitivity to inhibition. *Neuron* 85:573–589.
- Hummel T, Rodrigues V (2008) Development of the *Drosophila* olfactory system. *Adv Exp Med Biol* 628:82–101.
- Hummel T, Zipursky SL (2004) Afferent induction of olfactory glomeruli requires N-cadherin. *Neuron* 42:77–88.
- Ilieva H, Polymenidou M, Cleveland DW (2009) Non-cell autonomous toxicity in neurodegenerative disorders: ALS and beyond. *J Cell Biol* 187:761–772.
- Jarecki J, Keshishian H (1995) Role of neural activity during synaptogenesis in *Drosophila*. *J Neurosci* 15:8177–8190.
- Jefferis GSXE, Hummel T (2006) Wiring specificity in the olfactory system. *Semin Cell Dev Biol* 17:50–65.
- Jefferis GSXE, Marin EC, Stocker RF, Luo L (2001) Target neuron prespecification in the olfactory map of *Drosophila*. *Nature* 414:204–208.
- Jefferis GSXE, Vyas RM, Berdnik D, Ramaekers A, Stocker RF, Tanaka NK, Ito K, Luo L (2004) Developmental origin of wiring specificity in the olfactory system of *Drosophila*. *Development* 131:117–130.
- Jefferis GSXE, Potter CJ, Chan AM, Marin EC, Rohlffing T, Maurer CR, Luo L (2007) Comprehensive maps of *Drosophila* higher olfactory centers: spatially segregated fruit and pheromone representation. *Cell* 128:1187–1203.
- Keshishian H, Broadie K, Chiba A, Bate M (1996) The *Drosophila* neuromuscular junction: a model system for studying synaptic development and function. *Annu Rev Neurosci* 19:545–575.
- Kiss EA, Vonarbourg C, Kopfmann S, Hobeika E, Finke D, Esser C, Diefenbach A (2011) Natural aryl hydrocarbon receptor ligands control organogenesis of intestinal lymphoid follicles. *Science* 334:1561–1565.
- Kittel RJ, Wichmann C, Rasse TM, Fouquet W, Schmidt M, Schmid A, Wagh DA, Pawlu C, Kellner RR, Willig KI, Hell SW, Buchner E, Heckmann M, Sigrist SJ (2006) Bruchpilot promotes active zone assembly, Ca2+ channel clustering, and vesicle release. *Science* 312:1051–1054.
- Koch SC, Nelson A, Hartenstein V (2021) Structural aspects of the aging invertebrate brain. *Cell Tissue Res* 383:931–947.
- Komiyama T, Luo L (2006) Development of wiring specificity in the olfactory system. *Curr Opin Neurobiol* 16:67–73.
- Kremer MC, Christiansen F, Leiss F, Paehler M, Knapek S, Andlauer TFM, Förstner F, Kloppenburg P, Sigrist SJ, Tavosanis G (2010) Structural long-term changes at mushroom body input synapses. *Curr Biol* 20:1938–1944.
- Kummer TT, Misgeld T, Sanes JR (2006) Assembly of the postsynaptic membrane at the neuromuscular junction: paradigm lost. *Curr Opin Neurobiol* 16:74–82.
- Kurtovic A, Widmer A, Dickson BJ (2007) A single class of olfactory neurons mediates behavioural responses to a *Drosophila* sex pheromone. *Nature* 446:542–546.
- Laissue PP, Reiter C, Hiesinger PR, Halter S, Fischbach KF, Stocker RF (1999) Three-dimensional reconstruction of the antennal lobe in *Drosophila melanogaster*. *J Comp Neurol* 405:543–552.
- Lee PR, Fields RD (2021) Activity-dependent gene expression in neurons. *Neuroscientist* 27:355–366.
- Lee T, Luo L (1999) Mosaic analysis with a repressible cell marker for studies of gene function in neuronal morphogenesis. *Neuron* 22:451–461.
- Li A, Rao X, Zhou Y, Restrepo D (2020) Complex neural representation of odour information in the olfactory bulb. *Acta Physiol (Oxf)* 228:e13333.
- Li L, Xiong WC, Mei L (2018) Neuromuscular junction formation, aging, and disorders. *Annu Rev Physiol* 80:159–188.
- Li M, Cui Z, Niu Y, Liu B, Fan W, Yu D, Deng J (2010) Synaptogenesis in the developing mouse visual cortex. *Brain Res Bull* 81:107–113.
- Lin DM, Goodman CS (1994) Ectopic and increased expression of fasciclin II alters motoneuron growth cone guidance. *Neuron* 13:507–523.
- Liou NF, Lin SH, Chen YJ, Tsai KT, Yang CJ, Lin TY, Wu TH, Lin HJ, Chen YT, Gohl DM, Silies M, Chou YH (2018) Diverse populations of local interneurons integrate into the *Drosophila* adult olfactory circuit. *Nat Commun* 9:2232.
- Liu W, Chakkalakal JV (2018) The composition, development, and regeneration of neuromuscular junctions. *Curr Top Dev Biol* 126:99–124.
- Liu KSYY, Siebert M, Mertel S, Knoche E, Wegener S, Wichmann C, Matkovic T, Muhammad K, Depner H, Mettke C, Bückers J, Hell SW, Müller M, Davis GW, Schmitz D, Sigrist SJ (2011) RIM-binding protein, a central part of the active zone, is essential for neurotransmitter release. *Science* 334:1565–1569.
- Martin F, Boto T, Gomez-Diaz C, Alcorta E (2013) Elements of olfactory reception in adult *Drosophila melanogaster*. *Anat Rec (Hoboken)* 296:1477–1488.
- Masland RH (2004) Neuronal cell types. *Curr Biol* 14:R497–R500.
- Miech C, Pauer HU, He X, Schwarz TL (2008) Presynaptic local signaling by a canonical wingless pathway regulates development of the *Drosophila* neuromuscular junction. *J Neurosci* 28:10875–10884.
- Miller KD (1996) Synaptic economics: competition and cooperation in synaptic plasticity. *Neuron* 17:371–374.
- Modi MN, Shuai Y, Turner GC (2020) The *Drosophila* mushroom body: from architecture to algorithm in a learning circuit. *Annu Rev Neurosci* 43:465–484.
- Mosca TJ, Luo L (2014) Synaptic organization of the *Drosophila* antennal lobe and its regulation by the Teneurins. *Elife* 3:e03726.
- Mosca TJ, Luginbuhl DJ, Wang IE, Luo L (2017) Presynaptic LRP4 promotes synapse number and function of excitatory CNS neurons. *Elife* 6:115907.
- Mullins C, Fishell G, Tsien RW (2016) Unifying views of autism spectrum disorders: a consideration of autoregulatory feedback loops. *Neuron* 89:1131–1156.
- Ng M, Roorda RD, Lima SQ, Zemelman BV, Morcillo P, Miesenböck G (2002) Transmission of olfactory information between three populations of neurons in the antennal lobe of the fly. *Neuron* 36:463–474.
- Nitabach MN, Wu Y, Sheeba V, Lemon WC, Strumbos J, Zelensky PK, White BH, Holmes TC (2006) Electrical hyperexcitation of lateral ventral pacemaker neurons desynchronizes downstream circadian oscillators in the fly circadian circuit and induces multiple behavioral periods. *J Neurosci* 26:479–489.
- Nitkin RM, Smith MA, Magill C, Fallon JR, Yao YM, Wallace BG, McMahan UJ (1987) Identification of agrin, a synaptic organizing protein from torpedo electric organ. *J Cell Biol* 105:2471–2478.
- Pan Y, Monje M (2020) Activity shapes neural circuit form and function: a historical perspective. *J Neurosci* 40:944–954.
- Petzoldt AG, Götz TWB, Driller JH, Lützkendorf J, Reddy-Alla S, Matkovic-Rachid T, Liu S, Knoche E, Mertel S, Ugorets V, Lehmann M, Ramesh N, Beuschel CB, Kuropka B, Freund C, Stelzl U, Loll B, Liu F, Wahl MC,

- Sigrist SJ (2020) RIM-binding protein couples synaptic vesicle recruitment to release sites. *J Cell Biol* 219:e201902059.
- Potter CJ, Tasic B, Russler EV, Liang L, Luo L (2010) The Q system: a repressible binary system for transgene expression, lineage tracing, and mosaic analysis. *Cell* 141:536–548.
- Ren D, Navarro B, Xu H, Yue L, Shi Q, Clapham DE (2001) A prokaryotic voltage-gated sodium channel. *Science* 294:2372–2375.
- Sakano H (2020) Developmental regulation of olfactory circuit formation in mice. *Dev Growth Differ* 62:199–213.
- Sakuma C, Anzo M, Miura M, Chihara T (2014) Development of olfactory projection neuron dendrites that contribute to wiring specificity of the *Drosophila* olfactory circuit. *Genes Genet Syst* 89:17–26.
- Sanes JR, Lichtman JW (1999) Development of the vertebrate neuromuscular junction. *Annu Rev Neurosci* 22:389–442.
- Schlegel P, Bates AS, Stürmer T, Jagannathan SR, Drummond N, Hsu J, Serratos Capdevila L, Javier A, Marin EC, Barth-Maron A, Tamimi IF, Li F, Rubin GM, Plaza SM, Costa M, Jefferis GSXE (2021) Information flow, cell types and stereotypy in a full olfactory connectome. *Elife* 10:e66018.
- Schmid A, Hallermann S, Kittel RJ, Khorramshahi O, Frölich AMJ, Quentin C, Rasse TM, Mertel S, Heckmann M, Sigrist SJ (2008) Activity-dependent site-specific changes of glutamate receptor composition in vivo. *Nat Neurosci* 11:659–666.
- Seki Y, Dweck HKM, Rybak J, Wicher D, Sachse S, Hansson BS (2017) Olfactory coding from the periphery to higher brain centers in the *Drosophila* brain. *BMC Biol* 15:56.
- Sethi S, Lin H-H, Shepherd AK, Volkan PC, Su C-Y, Wang JW (2019) Social Context Enhances Hormonal Modulation of Pheromone Detection in *Drosophila*. *Curr Biol* 29:3887–3898.e4.
- Shi L, Fu AKY, Ip NY (2012) Molecular mechanisms underlying maturation and maintenance of the vertebrate neuromuscular junction. *Trends Neurosci* 35:441–453.
- Siddiqui TJ, Craig AM (2011) Synaptic organizing complexes. *Curr Opin Neurobiol* 21:132–143.
- Simi A, Studer M (2018) Developmental genetic programs and activity-dependent mechanisms instruct neocortical area mapping. *Curr Opin Neurobiol* 53:96–102.
- Stocker RF, Lienhard MC, Borst A, Fischbach KF (1990) Neuronal architecture of the antennal lobe in *Drosophila melanogaster*. *Cell Tissue Res* 262:9–34.
- Stockinger P, Kvitsiani D, Rotkopf S, Tirián L, Dickson BJ (2005) Neural circuitry that governs *Drosophila* male courtship behavior. *Cell* 121:795–807.
- Südhof TC (2012) The presynaptic active zone. *Neuron* 75:11–25.
- Sugie A, Hakeda-Suzuki S, Suzuki E, Silies M, Shimoazono M, Möhl C, Suzuki T, Tavosanis G (2015) Molecular remodeling of the presynaptic active zone of *Drosophila* photoreceptors via activity-dependent feedback. *Neuron* 86:711–725.
- Suh GSB, Wong AM, Hergarden AC, Wang JW, Simon AF, Benzer S, Axel R, Anderson DJ (2004) A single population of olfactory sensory neurons mediates an innate avoidance behaviour in *Drosophila*. *Nature* 431:854–859.
- Suzuki Y, Schenk JE, Tan H, Gaudry Q (2020) A population of interneurons signals changes in the basal concentration of serotonin and mediates gain control in the *Drosophila* antennal lobe. *Curr Biol* 30:1110–1118.e4.
- Sweeney ST, Broadie K, Keane J, Niemann H, O’Kane CJ (1995) Targeted expression of tetanus toxin light chain in *Drosophila* specifically eliminates synaptic transmission and causes behavioral defects. *Neuron* 14:341–351.
- Tanaka NK, Tanimoto H, Ito K (2008) Neuronal assemblies of the *Drosophila* mushroom body. *J Comp Neurol* 508:711–755.
- Tanaka NK, Ito K, Stopfer M (2009) Odor-evoked neural oscillations in *Drosophila* are mediated by widely branching interneurons. *J Neurosci* 29:8595–8603.
- Tanaka NK, Endo K, Ito K (2012) Organization of antennal lobe-associated neurons in adult *Drosophila melanogaster* brain. *J Comp Neurol* 520:4067–4130.
- Thummel CS (2001) Molecular mechanisms of developmental timing in *C. elegans* and *Drosophila*. *Dev Cell* 1:453–465.
- Vonhoff F, Keshishian H (2017) Activity-dependent synaptic refinement: new insights from *Drosophila*. *Front Syst Neurosci* 11:23.
- Vosshall LB, Wong AM, Axel R (2000) An olfactory sensory map in the fly brain. *Cell* 102:147–159.
- Wagh DA, Rasse TM, Asan E, Hofbauer A, Schwenkert I, Dürrbeck H, Buchner S, Dabauvalle M-CC, Schmidt M, Qin G, Wichmann C, Kittel R, Sigrist SJ, Buchner E (2006) Bruchpilot, a protein with homology to ELKS/CAST, is required for structural integrity and function of synaptic active zones in *Drosophila*. *Neuron* 49:833–844.
- White BH, Osterwalder TP, Yoon KS, Joiner WJ, Whim MD, Kaczmarek LK, Keshishian H (2001) Targeted attenuation of electrical activity in *Drosophila* using a genetically modified K(+) channel. *Neuron* 31:699–711.
- Wilson RI (2013) Early olfactory processing in *Drosophila*: mechanisms and principles. *Annu Rev Neurosci* 36:217–241.
- Wilton DK, Dissing-Olesen L, Stevens B (2019) Neuron-glia signaling in synapse elimination. *Annu Rev Neurosci* 42:107–127.
- Woźnicka O, Görlich A, Sigrist S, Pyza E (2015) BRP-170 and BRP190 isoforms of Bruchpilot protein differentially contribute to the frequency of synapses and synaptic circadian plasticity in the visual system of *Drosophila*. *Front Cell Neurosci* 9:238.
- Wu JS, Luo L (2006) A protocol for dissecting *Drosophila melanogaster* brains for live imaging or immunostaining. *Nat Protoc* 1:2110–2115.
- Wu H, Xiong WC, Mei L (2010) To build a synapse: signaling pathways in neuromuscular junction assembly. *Development* 137:1017–1033.
- Yaksi E, Wilson RI (2010) Electrical coupling between olfactory glomeruli. *Neuron* 67:1034–1047.
- Zeng H, Sanes JR (2017) Neuronal cell-type classification: challenges, opportunities and the path forward. *Nat Rev Neurosci* 18:530–546.
- Zhuang L, Sun Y, Hu M, Wu C, La X, Chen X, Feng Y, Wang X, Hu Y, Xue L (2016) Or47b plays a role in *Drosophila* males’ preference for younger mates. *Open Biol* 6:160086.